Coupling a water balance model with forest inventory data to predict drought stress: the role of forest structural changes vs. climate changes

Miquel De Cáceres[1,2,*], Jordi Martínez-Vilalta[2,3], Lluís Coll[1,2], Pilar Llorens[4], Pere Casals[1], Rafael Poyatos[2], Juli G. Pausas[5], Lluís Brotons[1,2,6]

[1]*InForest Joint Research Unit, CTFC-CEMFOR, Solsona, 25280, Spain;*

[2]*CREAF, Cerdanyola del Vallès, 08193, Spain;*

[3]*Universitat Autònoma de Barcelona, Cerdanyola del Vallès, 08193, Spain;*

[4]*Institute of Environmental Assessment and Water Research (IDÆA-CSIC) Barcelona, 08034, Spain;*

[5]*Centro de Investigaciones sobre Desertificación (CIDE-CSIC), Valencia, Spain;*

[6]*CSIC, Cerdanyola del Vallès, 08193, Spain;*

[*] Corresponding author: Miquel De Cáceres, Centre Tecnològic Forestal de Catalunya. Ctra. antiga St. Llorenç km 2, E-25280 – Solsona, Catalonia, Spain. E-mail: miquelcaceres@gmail.com. Fax: (+34) 973 48 13 92.

This is the author's version of a work that was accepted for publication in Agricultural and forest meteorology (Ed. Elsevier). Changes resulting from the publishing process, such as peer review, editing, corrections, structural formatting, and other quality control mechanisms may not be reflected in this document. Changes may have been made to this work since it was submitted for publication. A definitive version was subsequently published in De Cáceres, M., et al. “Coupling a water balance model with forest inventory data to predict drought stress : the role of forest structural changes vs. climate changes” in Agricultural and forest meteorology, vol. 213 (Nov. 2015), p. 77-90. DOI 10.1016/j.agrformet.2015.06.012

Abstract

Mechanistic water balance models can be used to predict soil moisture dynamics and drought stress in individual forest stands. Predicting current and future levels of plant drought stress is important not only at the local scale, but also at larger, landscape to regional, scales, because these are the management scales at which adaptation and mitigation strategies are implemented. To obtain reliable predictions of soil moisture and plant drought stress over large extents, water balance models need to be complemented with detailed information about the spatial variation of vegetation and soil attributes. We designed, calibrated and validated a water balance model that produces annual estimates of drought intensity and duration for all plant cohorts in a forest stand. Taking Catalonia (NE Spain) as a case study, we coupled this model with plot records from two Spanish forest inventories in which species identity, diameter and height of plant cohorts were available. Leaf area index of each plant cohort was estimated from basal area using species-specific relationships. Vertical root distribution for each species in each forest plot was estimated by determining the distribution that maximized transpiration in the model, given average climatic conditions, soil attributes and stand density. We determined recent trends (period 1980-2010) in drought stress for the main tree species in Catalonia; where forest growth and densification occurs in many areas as a result of rural abandonment and decrease of forest management. Regional increases in drought stress were detected for most tree species, although we found high variation in stress changes among individual forest plots. Moreover, predicted trends in tree drought stress were mainly due to changes in leaf area occurred between the two forest inventories rather than to climatic trends. We conclude that forest structure needs to be explicitly considered in assessments of plant drought stress patterns and trends over large geographic areas,

and that forest inventories are useful sources of data provided that reasonably good estimates of soil attributes and root distribution are available. Our approach coupled with recent improvements in forest survey technologies may allow obtaining spatially continuous and precise assessments of drought stress. Further efforts are needed to calibrate drought-related demographic processes before water balance and drought stress estimates can be fully used for the accurate prediction of drought impacts.

Keywords: Drought stress, forest inventory data, Mediterranean forests, water balance model.

Abbreviations: DDS – Daily drought stress; DI – Drought intensity; NDD – Number of drought days; LAI – Leaf area index; PET – Potential evapotranspiration; SFI – Spanish forest inventory.

1. Introduction

Drought stress is a key factor to understand the dynamics of most terrestrial ecosystems worldwide. Although drought impacts are often progressive and cumulative, reports of large-scale events of drought-related forest decline are increasingly common and have been linked to on-going global warming (Allen et al., 2010; Carnicer et al. 2011). Being able to anticipate where, when and which plant species will be impacted by cumulative drought or extreme drought events is particularly important at landscape to regional scales, because strategies focusing on adaptation and mitigation of drought impacts are normally designed and implemented at these scales (e.g., Lindner et al., 2010).

Assessments of plant drought stress can be obtained using a range of approaches differing in the drought definition, the spatial and temporal resolution, the degree of complexity and the amount of information required (Dai, 2011; Heim, 2002). While meteorological drought is routinely quantified using indices that employ temperature and precipitation data obtained from ground meteorological stations (e.g., McKee et al., 1993; Palmer, 1965; Vicente-Serrano et al., 2010), soil moisture, vegetation stress and decline are usually monitored for large areas using indices derived from satellite remote sensing (e.g., Deshayes et al. 2006; Gao, 1996; Gobron et al., 2005; Kerr et al., 2012; Kogan, 1997). An alternative, or complementary, way of estimating drought stress is by using process-based models that, given some meteorological, edaphic and vegetation data, are able to predict temporal variations of soil moisture and plant drought stress (e.g., Granier et al., 2007; Lafont et al., 2012; Ruffault et al., 2013). Compared to drought monitored by remote sensing, process-based models have the advantage of allowing drought stress to be explicitly differentiated from other factors affecting plant health condition, such as pests, diseases or air pollution (Deshayes et

78 al., 2006). Moreover, they allow future drought stress impacts to be anticipated when
79 coupled with climatic projections (e.g., Ruffault et al., 2014).

80 Different kinds of process-based models (e.g., hydrological models, ecosystem
81 models, forest gap models, landscape dynamics models or dynamic global vegetation
82 models) include modules to calculate soil water balance (e.g., Bugmann & Cramer
83 1998; Davi et al., 2005; Dufrêne et al., 2005; Lischke et al., 2006; Martínez-Vilalta et
84 al., 2002; Mouillot et al., 2001; Running & Coughlan, 1988; Sitch et al., 2003; Sus et
85 al., 2014) and, hence, can be used to track temporal variation in drought stress. These
86 models often differ in spatial resolution and the amount of detail of the representation
87 of soil and vegetation. They also differ in the representation of processes related to
88 water fluxes and drought stress (i.e., meteorological, hydrological, physiological or
89 demographic processes).

90 Although many process-based models include more or less detailed soil water
91 balance calculations, not all models are equally suited to obtain species-specific maps
92 showing drought stress over entire landscapes or regions. Since plant species differ in
93 their strategy to cope with drought and their ability to extract water at different soil
94 water potentials, the design of the chosen model should be able to simulate the
95 competition of plant cohorts and species for local water resources (e.g., Mouillot et
96 al., 2001). Moreover, the definition of state variables should include leaf area, or a
97 close surrogate, because the leaf area of a stand strongly influences soil moisture
98 dynamics and, in turn, the intensity and duration of drought stress (e.g., Joffre &
99 Rambal, 1993). Finally, the application of a model with very detailed representation
100 of processes may be constrained for landscape and regional applications by the high
101 number of parameters required. Such extensive applications are better approached

using a simpler but robust model easy to parameterize for a broad range of environmental conditions (Ruffault et al., 2014, 2013).

Assessing plant drought stress over landscapes and regions using process-based models requires detailed spatial information of soil and vegetation attributes. While not spatially continuous, the systematic sampling and repeated surveys of national forest inventories allow the forest structure and composition to be monitored for large geographic areas. Data from forest inventories have already been used in combination with ecosystem models to predict primary production and water and carbon fluxes over landscapes and regions (e.g., Keenan et al., 2011; Le Maire et al., 2005). However, the design of the models employed in these exercises did not allow distinguishing the drought stress of cohorts and species coexisting in forest plots. This level of detail in drought stress assessments is important, for example, for assisting management decisions aimed to improve the resilience of forests in front of drought impacts. Moreover, species-specific drought stress assessments are a key component of landscape simulation models aimed at anticipating the effects of drought in combination with other drivers such as wildfires or insect outbreaks (e.g., Fyllas and Troumbis, 2009; Gustafson and Sturtevant, 2013).

In this paper we explore the potential advantages and limitations of coupling forest inventory data with a water balance model to monitor the amount of drought stress experienced by plant species over large areas. We first present the design, parameterization and validation of a water balance model that allows tracking soil moisture variations and quantifying drought stress for plant cohorts (of the same or different species) in forest stands. The state base of the model is adapted for its use in combination with forest inventory data, whereas the complexity in terms of processes is kept very simple to reduce the number of parameters and facilitate its application to

different areas. We use Catalonia (NE Spain) as a case study and take the Second and Third Spanish National Forest Inventories in that region as source of vegetation structure and composition data for the water balance model. After estimating leaf area indices and vertical root distribution for each plant cohort in each forest plot, we examine two other issues that may compromise the use of this approach. First, we ask to what extent incomplete knowledge regarding soil depth may preclude obtaining accurate predictions of drought stress. Second, by comparing the predictions obtained using the two forest inventories, we determine to what extent local and regional-average drought stress assessments may be biased when conducted several years after a given survey. Finally, we illustrate our approach by determining recent temporal trends (1980-2010) in drought stress for the main tree species in the study area. Our hypothesis in this application is that vegetation changes occurred during this period should explain an important part of the variability in drought stress. Hence, we distinguish between the effect of climatic variations and the effect of changes in vegetation structure.

2. Materials and methods

2.1 Water balance model and drought stress definition

The purpose of the water balance model is to predict temporal variations in soil water content and assess drought stress for plants in a forest. Our model follows the design principles of BILJOU (Granier et al., 1999, 2007) and SIERRA (Mouillot et al., 2001; Ruffault et al., 2014, 2013), with some characteristics taken from dynamic global vegetation models (Prentice et al., 1993). The model calculates water balance on a daily basis. Soil is represented using two layers – topsoil and subsoil – and the model keeps track of the proportion of moisture relative to field capacity for each layer. Soil

151 water holding capacity includes the effects of rock fragment content. Vegetation is
152 represented as a set of plant cohorts having different height, root distribution, species
153 identity and leaf area index (LAI; i.e. the one-side area of leaves corresponding to the
154 cohort per unit of stand surface area). The root system of each cohort is described by
155 the vertical distribution of its fine root biomass, calculated following the linear dose
156 response model (Schenk and Jackson, 2002) (see section 2.6 and Appendix S1). The
157 minor fraction of root mass located below soil depth is redistributed within the
158 existing layers and the proportion of fine roots in each soil layer is assumed
159 proportional to the amount of water extracted from it.

160 Every day the model first updates leaf area of (semi-)deciduous plants according
161 to a simple phenological model that determines leaf budburst and leaf fall, where
162 parameter S_{GDD} indicates the growth degree days necessary for budburst (evergreen
163 plants are assumed to have constant leaf area throughout the simulation). Then, the
164 model recalculates light extinction through the canopy, following the Beer-Lambert
165 model, and the water storage capacity of the canopy (i.e. the minimum amount of
166 water needed to saturate the canopy). Species-specific parameters needed for these
167 calculations are the light extinction coefficient (k_{sp}), the bole height proportion (b_{sp})
168 and the canopy water storage capacity per LAI unit (s_{sp}). After updating the canopy
169 status, the model deals with the water input from rainfall. Before increasing the water
170 content of soil layers, the model first subtracts the water lost due to interception and
171 the water lost through surface runoff from rainfall. Rainfall interception loss is
172 estimated using the sparse version of the Gash model (Gash et al., 1995) and runoff is
173 estimated using the USDA SCS curve number method according to Boughton (1989).
174 Lateral water transfer processes are not considered. Soil water storage capacity and
175 water potential are calculated from texture using pedotransfer functions (Saxton et al.,

1986). When refilling a given soil layer, a proportion of water is assumed to directly percolate to the next layer below, as dictated by macroporosity (Granier et al., 1999). The water percolating from the deepest layer is assumed to be lost via deep drainage.

After refilling soil layers, the model determines evapotranspiration losses. Daily potential evapotranspiration (PET) is determined following the theory of equilibrium evapotranspiration (Jarvis and McNaughton, 1986; Prentice et al., 1993). Evaporation from the soil surface is controlled by PET, the amount of light reaching the ground and the water content of the topsoil, but the reduction in moisture is divided among the two soil layers according to a negative exponential function (Ritchie, 1972). To determine plant transpiration, the model first determines the maximum transpiration of the whole stand (i.e. assuming that water is not limiting) as a function of the stand's LAI and PET (Granier et al., 1999). Following Mouillot et al. (2001), the amount of water extracted by a plant cohort from a given soil layer is defined as the product of: (i) the maximum transpiration of the stand; (ii) the proportion of maximum transpiration that corresponds to the plant cohort, calculated on the basis of its leaf area and the amount of light available to it; (iii) the relative whole-plant conductance corresponding to the water potential in the soil layer; (iv) the proportion of fine roots in the soil layer. Relative whole-plant conductance lies between 0% (no conductance) and 100% (maximum conductance) and depends on the water potential in the soil layer and Ψ_{sp}, the species-specific water potential corresponding to 50% loss of conductance. Ψ_{sp} is a model parameter that integrates all the processes that may affect whole-plant water conductance, including stomatal regulation, xylem embolism and changes at the soil-root interface (Sperry et al., 1998; Martínez-Vilalta et al., 2014). Therefore, its interpretation may differ depending on the behavior of the species under drought (e.g., McDowell et al., 2008). For relatively isohydric species Ψ_{sp} would

mostly reflect the soil water potential associated to stomata closure, whereas for relatively anisohydric species Ψ_{sp} may be controlled by their vulnerability to xylem embolism.

Granier (1999) and Granier et al. (2007) defined drought stress to begin when soil relative extractable water was below 40%, whereas in Ruffault et al. (2014, 2013) drought periods start when soil water potential drops below – 0.5 MPa (a value beyond which a decrease in canopy conductance is observed for many Mediterranean species; Limousin et al., 2009). Following Mouillot et al. (2002), we defined drought stress periods for a given plant cohort as periods when relative whole-plant conductance is below 50%. Daily drought stress (*DDS*) of a plant cohort is defined as the one-complement of the relative conductance integrated across soil layers (Collins & Bras, 2007):

$$DDS_i = \phi_i \cdot \sum_s (1 - K_{i,s}) \cdot v_{i,s} \quad (1)$$

where $K_{i,s}$ is the relative whole-plant conductance of cohort *i* in layer *s*; $v_{i,s}$ is the proportion of the fine roots that cohort *i* has in layer *s*; and ϕ_i is the cohort leaf-phenological status ($\phi_i \in [0,1]$), included to avoid winter deciduous plants from suffering drought stress during winter. We quantified annual drought duration as the number of drought days (*NDD*) with relative conductance below 50% (i.e. *DDS* > 0.5) and annual drought intensity (*DI*) as:

$$DI = \sum \max\left[\frac{0.5 - DDS}{0.5}, 0\right] / 365 \quad (2)$$

where *DI* is dimensionless and ranges between 0 (relative conductance always > 50%) and 1 (0% relative conductance during all year).

Additional details of the design and specific formulation of the water balance model are given in Appendix S1. Predicted drought intensity and duration are strongly sensitive to changes in annual rainfall and leaf area index, but other parameters like soil depth and root distribution also appear to be influential (see sensitivity analyses in Appendix S2). The model is implemented in C++ and is executed from an interface written in R language. An R package is available upon request to M. De Cáceres.

2.2 Study area and calibration of species-specific parameters

Catalonia (31144 km^2; northeast of Spain; Fig. 1) is a region with 60% of its surface covered by forests and shrublands. Prevailing climate in most of the region is Mediterranean, but strong climatic gradients occur as a result of complex relief and distance to the coast. Mean annual temperature ranges between –0.1 and +17 ºC (average +12.3ºC) and annual rainfall ranges between 344 and 1587 mm (average 684 mm). In most of the region, rainfall peaks in autumn and spring (average 222 and 194 mm, respectively), and it is relatively low during summer and winter (average 173 and 141 mm, respectively) (source: Ninyerola et al., 2000). In addition to the characteristic summer water deficit, Mediterranean climate often includes a strong inter-annual variation in rainfall and temperature regimes, which adds uncertainty to the intensity and duration of drought stress.

Fig. 1: Location of validation sites and forest inventory plots within Catalonia.

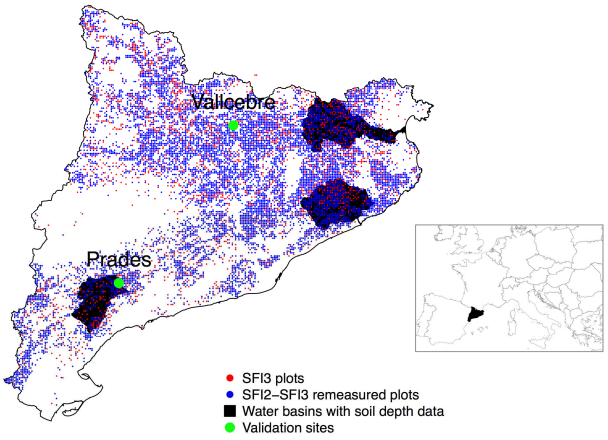

242

243 We treated the 12 most frequent tree species in the study area as separate
244 entities (see Table 1). Less frequent tree species were lumped together in a group
245 named 'other trees' and shrubs were divided into three functional groups related to
246 post-fire regeneration strategies (Keeley et al., 2012): 'Shrub R+S-' (resprouters),
247 'Shrub R-S+' (seeders) and 'Shrub R+S+' (facultative seeders). The full list of species
248 included in each group is given in Appendix S3. The proportion of bole height (b_{sp})
249 and light extinction coefficients (k_{sp}) for tree and shrub species were inferred from
250 bibliographic sources (Aubin et al., 2000; Bréda, 2003) (Table 1). To determine soil
251 water potentials related to 50% of water conductance loss, species were divided
252 between strongly isohydric (Ψ_{sp} = – 2.0 MPa; conifers, beech and 'other trees'),
253 moderately isohydric (Ψ_{sp} = – 3.0 MPa; oaks and 'shrubs R+S+'), moderately
254 anisohydric (Ψ_{sp} = – 4.0 MPa; 'shrubs R+S-') and strongly anisohydric (Ψ_{sp} = – 5.0
255 MPa; 'shrubs R-S+'). Considering the relatively high uncertainty in the Ψ_{sp} reflecting
256 in part methodological issues (e.g., Delzon and Cochard, 2014), we decided to group
257 species in 'functional types' to avoid generating artificial variability among species
258 and focusing on the differences that are robust enough to be interpretable. The Ψ_{sp}
259 values were established after examining and comparing several bibliographic sources:

(1) minimum recorded leaf water potentials for these species (Choat et al., 2012; Martínez-Vilalta et al., 2014); (2) water potentials causing 50% xylem embolism in stems (Choat et al. 2012); (3) water potentials at turgor loss point (Bartlett et al., 2012); and (4) water potentials at 50% stomatal closure (Klein, 2014). Values for s_{sp}, the amount of water that can be retained in the canopy of a particular species per LAI unit, were set after inspecting values reported in experimental studies. Additional information regarding the calibration of s_{sp} and Ψ_{sp} is included in Appendix S3.

Table 1: Species-specific model parameters and linear regressions used to estimate LAI. k_{sp} – Extinction coefficient, corresponding to global radiation in the case of trees (Bréda, 2003) and photosynthetic active radiation in the case of shrubs (Aubin et al. 2000); b_{sp} – bole height in relation to total height; s_{sp} – Canopy water storage capacity per LAI unit; Ψ_{sp} – Water potential associated to 50% conductance loss; S_{GDD} – Growth degree days (T_{base} = 5ºC) to attain full LAI. *LAI-BA* – estimated slope of the linear regression between basal area and LAI; *n* – number of observations; Range – range of basal area values considered; R^2adj – adjusted R-square.

Species / Functional group	k_{sp}	b_{sp} (%)	s_{sp} (mm·LAI^{-1})	Ψ_{sp} (MPa)	S_{GDD}	**LAI-BA**	**n**	**BA range** (m^2/ha)	**R^2adj**
Pinus halepensis	0.50	66	1.00	-2.0	–	0.05201	2712	[0.06, 51.39]	93.4 %
Pinus nigra	0.50	66	1.00	-2.0	–	0.06626	2063	[0.04, 67.82]	83.5%
Pinus sylvestris	0.50	66	1.00	-2.0	–	0.05213	3211	[0.04, 87.39]	94.2%
Pinus uncinata	0.50	66	1.00	-2.0	–	0.05061	787	[0.05, 82.15]	82.4%
Pinus pinea	0.50	66	1.00	-2.0	–	0.06293	985	[0.05, 48.2]	92.0%
Pinus pinaster	0.50	66	1.00	-2.0	–	0.05095	296	[0.06, 75.6]	82.9%
Abies alba	0.35	30	1.00	-2.0	–	0.10715	230	[0.3, 86.66]	95.3%
Quercus ilex	0.55	50	0.50	-3.0	–	0.14220	4063	[0.02, 56.68]	91.4%
Quercus suber	0.55	50	0.50	-3.0	–	0.03974	1032	[0.08, 62.28]	85.2%
Quercus humilis	0.55	50	0.50	-3.0	200	0.12481	1847	[0.03, 42.65]	91.4%
Quercus faginea	0.55	50	0.50	-3.0	200	0.14989	355	[0.04, 20.74]	72.2%
Fagus sylvatica	0.43	50	0.25	-2.0	200	0.12343	567	[0.07, 72.03]	83.3%
Other trees	0.43	50	0.25	-2.0	200	0.29178	180	[0.07, 14.86]	85.3%
Shrub R+S-	0.40	10	0.25	-4.0	–	0.19319	546	[0.03, 20.00]	92.2%
Shrub R-S+	0.40	10	0.25	-5.0	–	–	–	–	–
Shrub R+S+	0.40	10	0.25	-3.0	–	–	–	–	–

2.3 Model evaluation

We evaluated the predictive accuracy of the model with respect to variations in transpiration and soil water content using data from two distinct sites (Fig. 1). *Prades* site is characterized by a Mediterranean climate and has rocky and shallow soils. A

process of drought-induced decline of *P. sylvestris* is occurring in this site since the 1990s (Martínez-Vilalta and Piñol, 2002; Poyatos et al., 2013). *Vallcebre* site has a sub-Mediterranean climate and soils are deeper and with lower gravel content (Poyatos et al., 2005; Garcia-Estringana et al., 2013). We gathered soil and vegetation data for one stand in each site (Table 2). Soil attributes were determined from soil samples. As vegetation in *Prades* has been found to rely on deep water reserves during dry periods (Barbeta et al., 2014), we considered both the stand's measured soil depth (40 cm) as well as two additional parameterizations where soil field capacity was increased to account for the additional water volume potentially accessible through rock fissures and cracks (see Table 2). Tree leaf area for each species in each stand was calculated as a function of site-specific allometric relationships between stem/branch diameter and leaf mass/area. Root distribution was estimated by determining the parameters of the linear dose response function corresponding to maximum transpiration under average climatic conditions (see details in section 2.6).

Table 2: Site characteristics, model parameters employed and calculated drought stress for the two validation stands. Values within square brackets and braces for *Prades* indicate model parameters and drought stress values obtained after setting soil depth to 80 cm and considering an additional rocky layer (85% of rocks), respectively.

	Vallcebre	**Prades**
Location (coordinates)	42º12'N, 1º49'E	41º19'N, 1º1'E
Altitude (m a.s.l.)	1260	1015
Mean annual temperature (ºC)	7.3	11.3
Mean annual rainfall (mm)	862	664
Vegetation parameters		
Species	*Pinus sylvestris / Buxus sempervirens*	*P. sylvestris / Quercus ilex /* R+S-
Height	11 m / 2 m	14 m / 6 m / 2 m
LAI	2.4 / 0.3	0.54 / 2.69 / 0.2
Root volume in topsoil (%)	62 / 60	65 / 66 / 66 [74 / 74 / 69] {68 / 68 / 60}

k_{sp}	0.5/ 0.4	0.5 / 0.55 / 0.4
b_{sp} (%)	66 / 10	66 / 50 / 10
s_{sp} (mm·LAI^{-1})	1.0 / 0.25	1.0 / 0.5 / 0.25
Ψ_{sp} (MPa)	-2.0 / -4.0	-2.0 / -3.0 / -4.0
S_{GDD}	– / –	– / – / –
Soil parameters		
Soil depth (topsoil + subsoil)	65 cm (30 + 35 cm)	40 cm (30 + 10 cm) [80 cm (30 + 50 cm)] {80 cm + rocky layer down to 4.5 m}
Topsoil texture (% sand, silt, clay)	(59, 19, 22)	(47, 32, 21)
Topsoil bulk density (kg·dm^{-3})	1.23	0.98
Topsoil macroporosity (%)	27	33
Topsoil rock fragment content (%)	19	45
Subsoil texture (% sand, silt, clay)	(62, 20, 18)	(48, 33, 19)
Subsoil bulk density (kg·dm^{-3})	1.48	1.48
Subsoil macroporosity (%)	14	11
Subsoil rock fragment content (%)	19	51
Max. soil evaporation (mm·day^{-1})	1	2
Water volume at field capacity (mm)	122	54 [102]{238}
Predicted drought stress		
Average drought intensity (DI)	0.06 / 0.00	0.40 / 0.35 / 0.27 [0.33 / 0.27 / 0.17] {0.26 / 0.21 / 0.11}
Average drought duration (NDD)	32 / 0	151 / 141 / 128 [154 / 141 / 116] {148 / 133 / 97}

A three-year period (2003-2005 and 2011-2013 in *Vallcebre* and *Prades*, respectively) was used for validation and meteorological input data (daily temperature, rainfall and radiation) were obtained from on-site meteorological stations (Latron et al., 2010). Detailed descriptions regarding soil moisture and transpiration measurements for the validation period can be found in Poyatos et al. (2007), Poyatos et al. (2013), García-Estringana et al. (2013) and Sus et al. (2014). Predicted vs. observed values were compared using linear regression analyses.

2.4 Forest inventory data and LAI estimation

Surveys of the Second Spanish Forest Inventory (SFI2) were conducted in Catalonia between 1989 and 1991 (Villaescusa & Díaz, 1998), while those of the Third Spanish Forest Inventory (SFI3) were conducted between 2000 and 2001 (Villanueva 2004). SFI2 and SFI3 surveys include 11282 and 11454 forest plots, respectively. In this study we considered the 8977 plots that were sampled in both SFI2 and SFI3 (Fig. 1),

except for the determination of soil depth effects where we used all SFI3 plots located in areas where soil depth was available (see section 2.8).

In both surveys, forest plots had been divided into four nested circular subplots (radius 5, 10, 15 and 25 m); and trees had been recorded only if their diameter was larger than a threshold (7.5, 12.5, 22.5 and 42.5, respectively). Species identity, height and diameter at breast height (d.b.h.) of living and standing dead trees were available for both surveys. In the circular plot of 5 m radius, the number of saplings per species (2.5 cm $\leq$ d.b.h. < 7.5 cm) and their mean height had also been recorded. Species identity, canopy cover and mean height of woody understory vegetation had been sampled within the 10-m radius plot.

We assumed that each tree or shrub record was representative of a distinct plant cohort. Species identity and plant height, two parameters required in the model, were directly available from plot records. In order to obtain LAI estimates for trees, we calculated the basal area of each tree cohort and multiplied it by the slope of a species-specific linear regression with zero intercept against basal area (Table 1; see also Fig. S3.1 in Appendix S3), calibrated using data from Burriel et al. (2004). For shrubs, cover values were simply multiplied by 0.02 (i.e., 100% cover equals to LAI = 2). Estimation of root distribution is explained in section 2.6.

2.5 Climatic and soil data

Temperature (in ºC), rainfall (in mm) and mean daily solar radiation (in $10kJ \cdot m^{-2} \cdot day^{-1}$) data, spatially interpolated at 1 km resolution (Ninyerola et al., 2000), were obtained for each month in the 1980-2010 period from the Spanish Meteorological Agency (AEMET) and the Catalan Meteorological Service (SMC). Daily temperature and daily solar radiation were simply interpolated linearly between average monthly

values, whereas daily rainfall values were generated by sequentially drawing values from a Gamma distribution (shape = 2, scale = 4) until the monthly precipitation demand was met (model sensitivity to parameters of this distribution is included in Appendix S2). The ratio between the evaporation rate and the rainfall rate (a parameter needed for rainfall interception loss; see Appendix S1) was set to 0.2 between December and June and to 0.05 between July and November (Miralles et al., 2010).

Soil was poorly characterized in SFI2; and field surveys of SFI3 only included qualitative descriptions of soil texture, litter content and surface rock abundance. The percentage of rocks in the surface of the plot was taken as a proxy of rock fragment content in the soil. Soil texture and bulk density corresponding to the topsoil and subsoil (0 – 30 cm and 30 – 100 cm) were obtained from spatial layers from the Harmonized World Soil Database (FAO/IIASA/ISRIC/ISS-CAS/JRC 2009). Bulk density and the percent of sand were used to calculate macroporosity (Stolf et al., 2011). While being a key parameter for water balance, soil depth varies strongly at fine scale and is difficult to estimate accurately. To avoid overestimation of drought stress, we took a conservative approach and set soil depth (topsoil + subsoil) to 100 cm for all forest inventory plots (but we compared stress estimates in areas with available soil depth data, see section 2.8).

2.6 Root distribution

Plant roots can be quite deep in semi-arid and Mediterranean ecosystems (Canadell et al., 1996; Schenk and Jackson, 2002). Although root architecture is species-specific, abiotic and biotic factors have a profound influence on root growth and structure (Casper and Jackson, 1997). Unfortunately, plant root systems are rarely sampled in forest inventories. We estimated root distribution among soil layers by finding the

distribution that maximized plant transpiration in the model (preliminary analyses in which drought stress was minimized gave similar results) (Collins and Bras, 2007; Kleidon and Heimann, 1998). In the linear dose response model the distribution of roots is governed by parameters D50 and D95, the depths above which 50% and 95% of root mass is located, respectively (Schenk and Jackson, 2002). We explored the same state-space used in Collins and Bras (2007) and determined the D50/D95 pair corresponding to a maximum transpiration over three years of model simulation.

We determined optimum root distribution for each forest plot and each species separately. In each case, we used a single plant cohort of the target species with a LAI value equal to the LAI of the whole stand (thus, we assumed optimum root systems to be independent of the identity of neighbors). The factors that influenced the optimum root distribution of a given species in a given plot were: (i) species-specific model parameters (Ψ_{sp}, but also s_{sp} because it influenced soil infiltration); (ii) the LAI of the target stand; (iii) climatic conditions, soil texture and rock fragment content in the target plot. Pseudo-daily meteorological data for the optimization process was generated using average monthly values obtained from the Catalan Digital Climatic Atlas (Ninyerola et al., 2000; Pons and Ninyerola, 2008).

2.7 Model runs

All simulations started with soil layers at field capacity. Although all plant cohorts compete for water resources in the model, we evaluated drought stress for tree species only. Since the model produces DI and NDD values at the plant cohort level, drought stress values corresponding to each species and plot were obtained by averaging the stress values of plant cohorts of the plot corresponding to the same species, using LAI values as weights. We accounted for uncertainty derived from the stochastic

388 generation of daily precipitation by averaging DI and NDD values across ten model
389 runs. Preliminary analyses indicated that ten replicates correspond to a standard error
390 of around 0.001 for the DI average and less than one day for the NDD average.

391 *2.8 Bias in drought stress estimates derived from assuming constant soil depth*

392 In our application of the model to Catalonia we assumed a constant soil depth of 100
393 cm for all forest plots. To quantify the bias in drought stress derived from a lack of
394 soil depth data in the study area, we used 1435 SFI3 plots located within three
395 catchments where soil depth estimates were available, including 347 SFI3 plots that
396 had not been surveyed in SFI2 (Fig. 1). Soil depth spatial layers in these catchments
397 had been obtained from local soil maps complemented with estimates of regression
398 models between soil profile data and soil units (CREAF/UPC/ETC/IRTA, 2011).
399 Drought stress predictions for the year of SFI3 survey (either 2000 or 2001) were
400 calculated assuming 100 cm soil depth and using actual soil depth estimates. Species
401 optimum root distributions were determined separately for both soil depths.

402 *2.9 Bias in drought stress estimates derived from temporal extrapolation*

403 Our approach to assess drought stress relies on static information about forest
404 structure and composition. Hence, drought stress estimates can have a substantial bias
405 when conducted several years after the year of forest survey. To measure the bias
406 derived from assuming constant structure and composition in forest plots, we took the
407 8977 re-measured plots and calculated DI and NDD predictions using SFI2 data for
408 the year of the SFI3 survey and compared them with those obtained using SFI3 data.
409 As before, species optimum root distributions were estimated separately for SFI2 and
410 SFI3, with the aim to emulate the plasticity of root systems to adapt to changes in
411 aboveground structure. An increase in drought stress between forest inventories was

412 expected as a result of tree growth and forest densification; whereas decreases in
413 drought stress were expected in stands subjected to decreases in basal area, for
414 example after management or natural disturbances. We calculated Spearman's rank
415 correlation to test the relationship between the difference in predicted drought stress
416 and the corresponding SFI3-SFI2 difference in stand's LAI.

417 *2.10 Temporal trends in climate and plant drought stress*

418 We characterized 1980-2010 temporal trends in mean annual temperature, annual
419 precipitation and climatic drought for all SFI3 plots. Climatic drought was calculated
420 using the Standardized Precipitation-Evapotranspiration Index (SPEI; Vicente-
421 Serrano et al., 2010; Beguería & Vicente-Serrano, 2013), a multiscalar index whose
422 calculation involves a monthly climatic water balance series. For SPEI calculations,
423 monthly PET was obtained adding the daily values used in the model and the scale of
424 the index was 12 months.

425 Using the water balance model and the 8977 re-measured plots, we
426 characterized trends in drought stress for each species by combining drought stress
427 predictions obtained using SFI2 data (1989-1999 period) and SFI3 data (1991-2010
428 period). Drought stress during the 1991-1999 period was defined as the average of
429 SFI2 and SFI3 predictions using weights that depended on the year (for example,
430 SFI2 and SFI3 predictions had 0.9 and 0.1 weights, respectively, for year 1991; and
431 the reverse weights were used for year 1999). With the aim to distinguish drought
432 stress changes driven by climate from changes derived from changes in LAI, we
433 compared the trends predicted as explained above with those obtained using SFI2 data
434 for the whole period (1980-2010). In all cases the Mann-Kendall trend test (Mann,
435 1945) was used to determine the statistical significance of trends (significance level

was set to $P = 0.05$) and the magnitude of the trend was assessed using the Theil-Sen approach (Sen, 1968).

3. Results

3.1 Model evaluation

Predicted daily canopy transpiration values in *Vallcebre* site matched reasonably well the transpiration estimation obtained from sap flow measurements ($a = 0.289$; $b = 0.831$; $r^2 = 0.61$), except during the summer 2003 drought (Fig. 2a). Predicted topsoil moisture variations also matched moderately well with both manual ($a = 0.010$; $b = 0.836$; $r^2 = 0.41$) and automatic ($a = 0.006$; $b = 0.951$; $r^2 = 0.57$) field measurements (Fig. 2a). Topsoil moisture predictions for *Prades* site were rather strongly correlated with field measurements ($a = 0.030$; $b = 0.835$; $r^2 = 0.69$). Canopy transpiration was clearly underestimated during drought periods when using 40 cm soil depth ($a = 0.429$; $b = 0.527$; $r^2 = 0.25$) (Fig. 2b). However, the fit to observed transpiration improved when increasing soil depth to 80 cm ($a = 0.265$; $b = 0.789$; $r^2 = 0.51$) or when considering an additional rocky layer (85% of rocks) extending down to 4.5 m ($a = 0.171$; $b = 0.886$; $r^2 = 0.62$). As expected, predicted drought stress was much higher in *Prades* than in *Vallcebre* (e.g., NDD = 151 vs. 32 days for *Pinus sylvestris*; Table 2).

454 **Fig. 2** Meteorological input (top), canopy transpiration (center) and topsoil moisture (bottom) at *Vallcebre* (a) and *Prades* (b) stands. Center and
455 bottom panels include the comparison between observed values (in gray) and model predictions (in black).

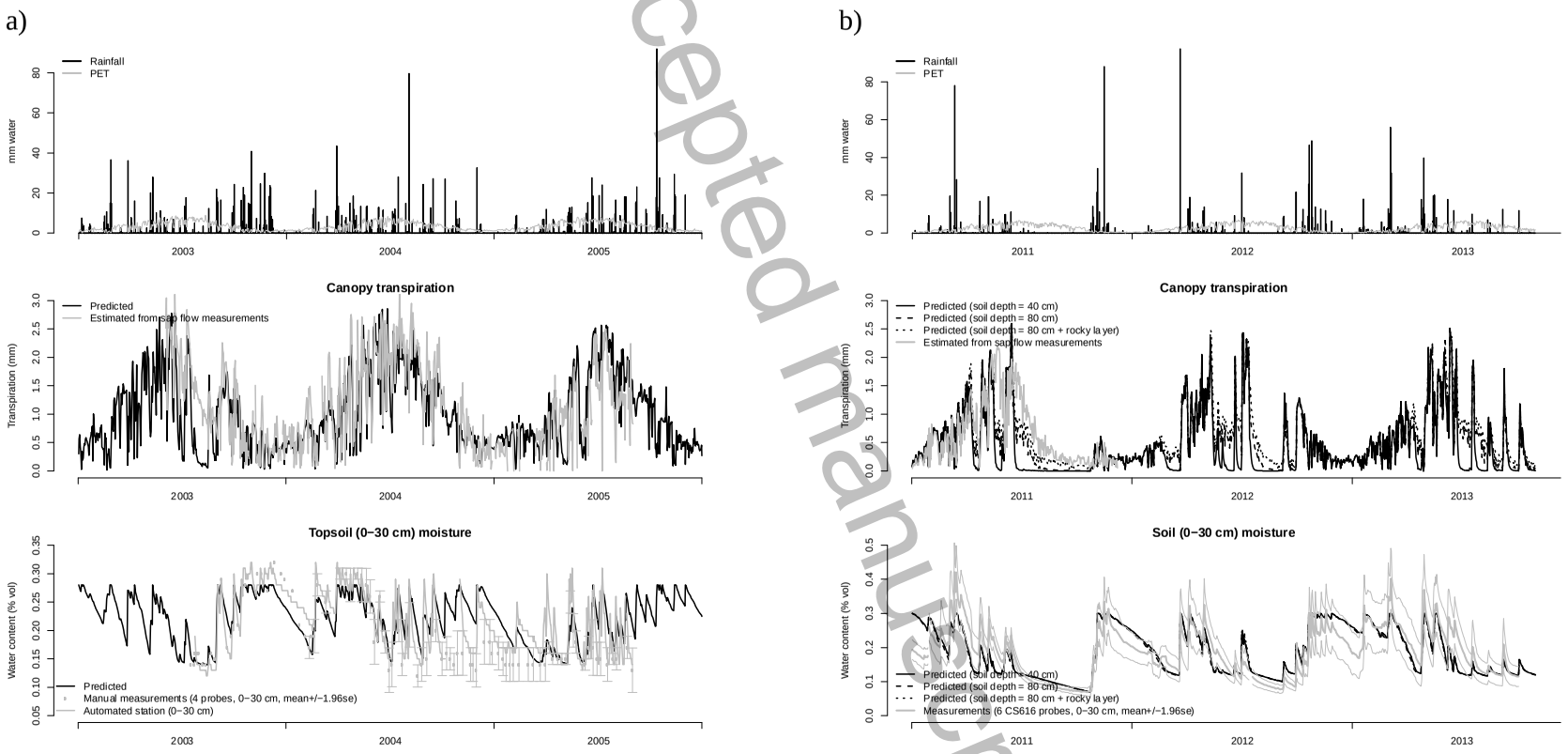

456

3.2 LAI and root distribution estimates

Stand LAI values were significantly smaller under SFI2 (mean = 1.8; s.d. = 1.4) than under SFI3 (mean = 2.0; s.d. = 1.4) [p-value < 0.0001 in a Wilcoxon test]; and differences in LAI were highly variable among stands (s.d. = 0.95) (Fig. 3).

Fig. 3: a) Density distribution of stand LAI values under SFI2 and SFI3, and distribution of LAI differences; b) Spatial distribution of LAI changes.

a) b)

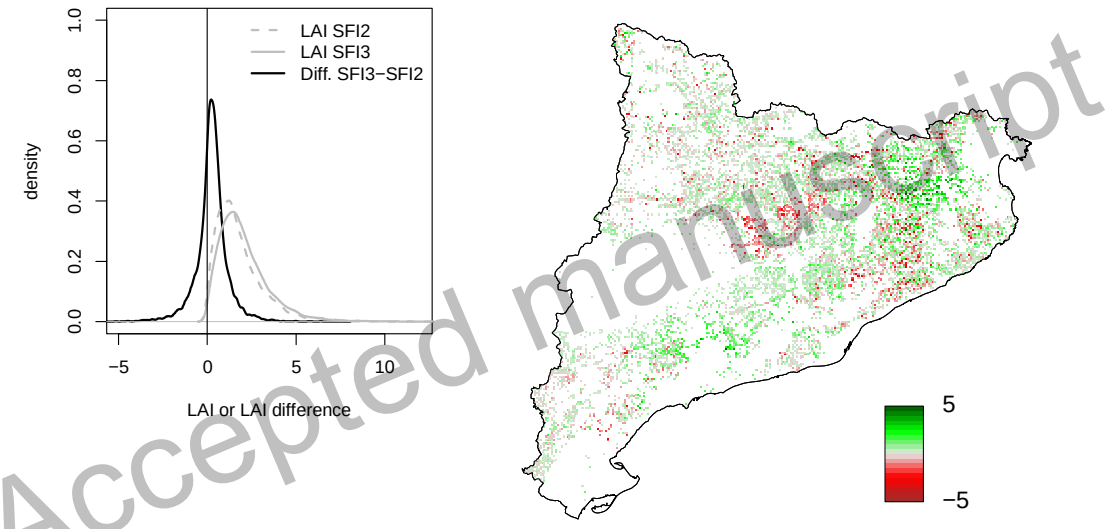

In plots with fine-textured soils root biomass tended to concentrate in the topsoil, whereas in medium- or coarse-textured soils roots were mostly in the subsoil (see Fig. S4.1 in Appendix S4). Under arid conditions differences in root distribution due to soil texture were relatively small. In contrast, when climatic wetness increased root distribution became shallower in fine-textured soils and deeper for other textures. The density of the stand also had a strong effect on root distribution.

3.3 Bias in drought stress estimates derived from assuming 100 cm soil depth

Soil depths were generally lower than 100 cm in the three catchments where estimates were available. Therefore, the model tended to underestimate water stress for those stands (Fig. 4). Although we found high variation among plots, on average drought stress bias was rather small for soils deeper than 50 cm (i.e., less than 0.05 in DI and less than 15 days in NDD) and it rapidly increased for shallower soils. A very small overestimation of drought stress occurred for soils deeper than 100 cm.

Fig. 4: Difference between drought stress values (DI and NDD) obtained assuming 100 cm soil depth for all plot records and drought stress values obtained using soil depth estimates available for three catchments (Fig. 1). N – Number of forest plots in each soil depth class.

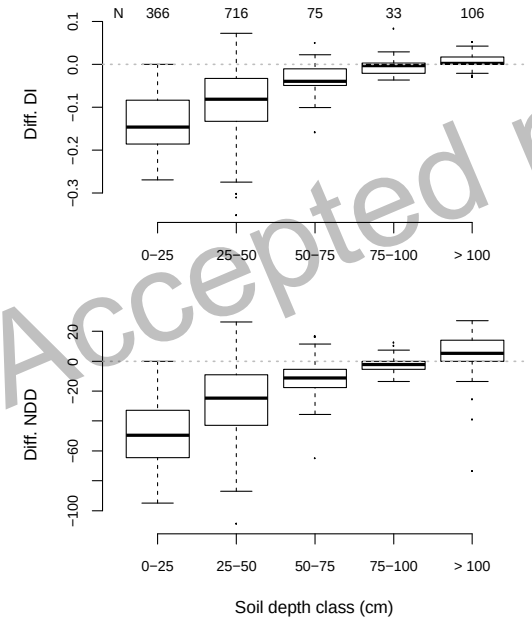

3.4. Bias in drought stress estimates derived from temporal extrapolation

For most species, the regional average SFI2-SFI3 difference in predicted drought stress was negative (Fig. 5), indicating an underestimation of stress for assessments conducted with SFI2 data. Specifically, regional average differences in NDD ranged

between –2 days and –17 days (corresponding to *P. uncinata* and *Q. humilis*, respectively) differences in DI ranged between –0.001 and –0.023 (corresponding to *P. uncinata* and *P. halepensis*, respectively).

Fig. 5: Differences between SFI2 and SFI3 in stand LAI (top), DI (center) and NDD (bottom). For each species, a boxplot shows the values of all plot records where the species is present. N – Number of forest plots where the species occurs; ρ – Spearman's correlation coefficient between differences in drought stress and differences in stand LAI.

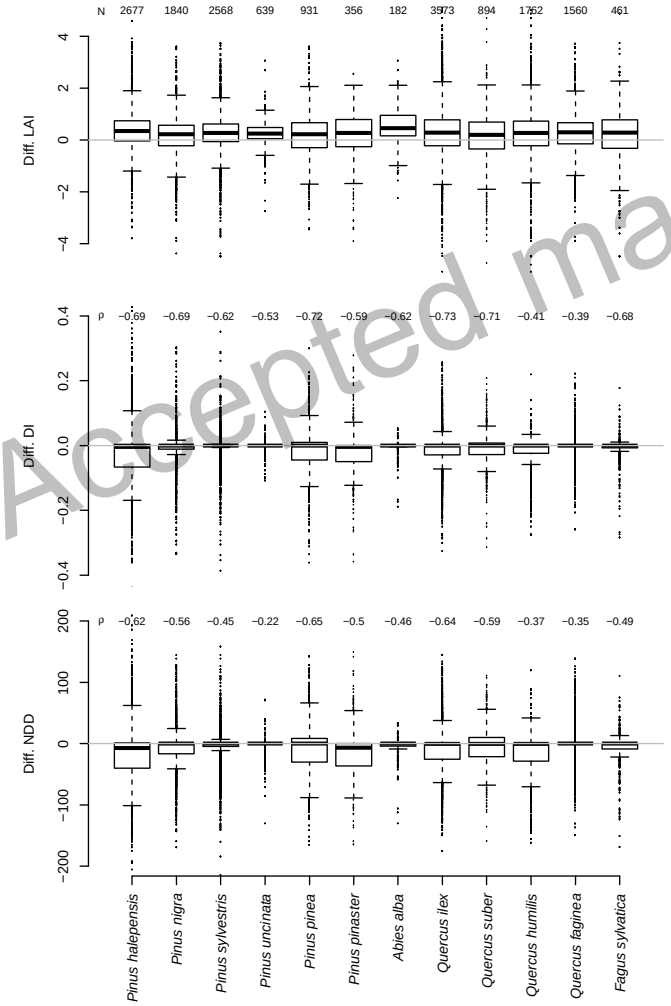

Drought stress differences varied strongly among forest plots; and correlations with changes in stand LAI were substantial (Spearman's ρ between –0.39 and –0.73 for DI and between –0.22 and –0.65 for NDD, depending on the species; Fig. 5). Among-plot variation in stand LAI differences was rather similar among species. In contrast, among-plot variation in drought stress changes between forest inventories was larger for Mediterranean species (*P. halepensis*, *P. pinea*, *P. pinaster*, *Q. ilex* and *Q. suber*) and progressively smaller for species corresponding to sub-Mediterranean (*P. nigra*, *Q. humilis* and *Q. faginea*), temperate (*P. sylvestris*, *F. sylvatica*, *A. alba*) and mountainous (*P. uncinata*) climates.

3.5 Temporal trends in climatic drought and tree drought stress in Catalonia

During the period 1980-2010, 42% of forest plots in the study area experienced significant increase in mean annual temperature; and only 0.2% experienced a decrease (mean change = +0.63 ºC; s.d. = 0.40 ºC) (Fig. 6a). In contrast, we found that only a few plots had experienced changes in annual precipitation (0.6% and 0.2% of plots with significant increase and decrease, respectively) and average precipitation changes in the region were relatively small (mean change = +11 mm, s.d. = 64 mm) (Fig. 6b). Regarding SPEI (scale = 12 months) we found a small tendency towards aridification (mean change = –0.13, s.d. = 0.45), with a significant aridification trend for 28.1% of plots and a significant decrease of aridity for 10.6% of plots (Fig. 6c).

The water balance model predicted an increase in drought stress during the period 1980-2010 for most tree species (Figs. 7-8), in accordance with the results obtained in subsection 3.4. For example, NDD increased for *Pinus halepensis* in 34% of the plots where the species was present while it decreased in 9% of plots. On average, annual drought duration increased in 17 days for this species, although with a

very large variability among plots (s.d. = 64 days). At the other extreme, NDD increased for *P. uncinata* for 4% of plots only, while it decreased for 0.5% of plots; and the average change in drought duration was a decrease of 1 day (s.d. = 10 days). Appendix S4 shows among-plot variation and the spatial distribution of both average drought stress and the magnitude of stress changes for the period studied.

When we determined trends in drought stress using SFI2 data alone (hence, assuming no change in forest structure during the studied period), we found very few changes in drought stress (between 0% to 1.7% of plots with an increase in NDD, and between 0% and 2.3% with an increase in DI, depending on the species) (Figs. 7-8). Moreover, changes in drought stress correlated moderately well with climatic changes when using SFI2 data alone; but they almost did not when both forest inventories were used. For example, Pearson's correlation between the 1980-2010 changes in SPEI and the corresponding changes in DI was $r = -0.40$ for *Q. ilex* when trends in DI were obtained assuming constant forest structure. In contrast, the same correlation was $r = -0.13$ when the change in forest structure was taken into account.

534 **Fig. 6:** Changes in mean annual temperature (MAT, in ºC), mean annual precipitation (MAP, in mm) and the Standardized Precipitation-

535 Evapotranspiration Index (SPEI, scale = 12 months) for the period 1980-2010. Trend analyses were conducted following the Theil-Sen approach.

a)

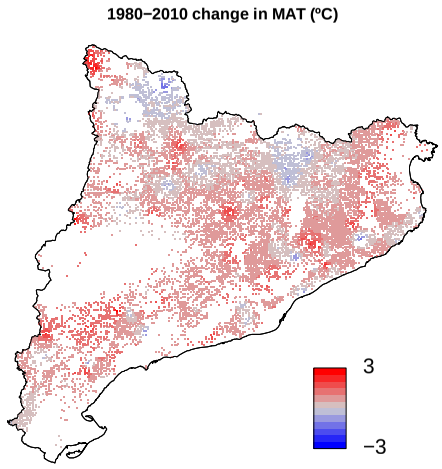

b)

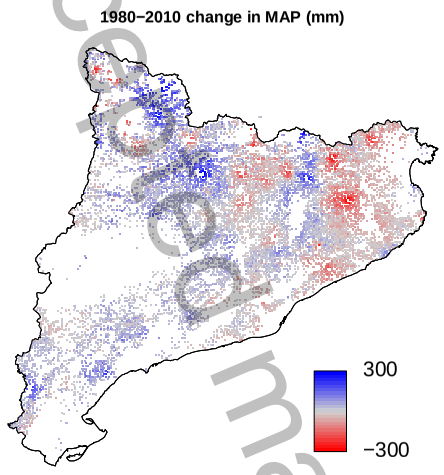

c)

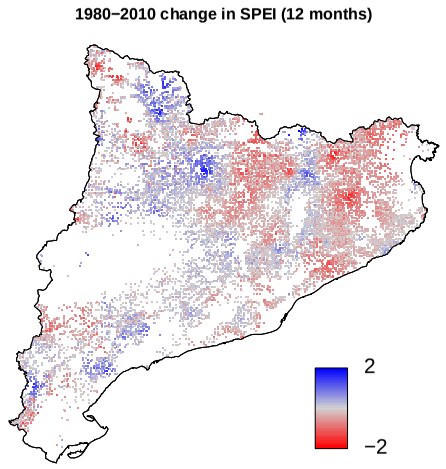

536

537

Fig. 7: Temporal trends in drought intensity (DI) for all studied species during the period 1980-2010. Red and blue lines indicate average trends calculated using SFI2 data or SFI3 data, respectively. Black lines indicate average trends obtained after combining predictions for both forest inventories. Trends for individual forest plots are shown in light grey. Change mean and s.d. – Mean and standard deviation of the magnitude of change in DI, according to the Theil-Sen approach. Incr./Decr. – Percentage of plots (among those where the species is present) with significant increase/decrease ($P < 0.05$) in DI, according to the Mann-Kendall trend test. Corr. SPEI – Pearson correlation between the slope of DI and the slope of Standardized Precipitation-Evapotranspiration Index (scale = 12 months).

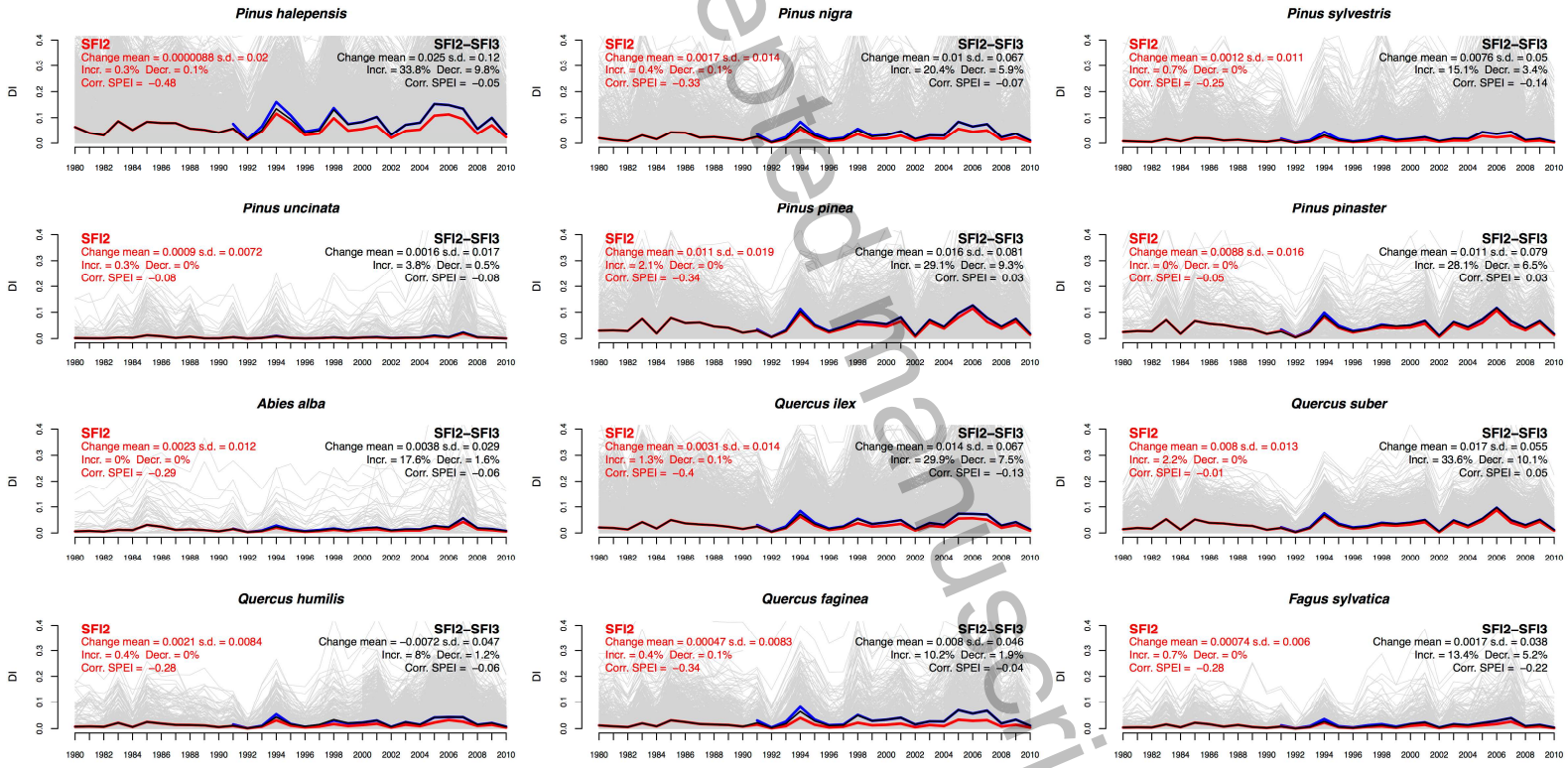

Fig. 8: Temporal trends in number of drought days (NDD) for all studied species during the period 1980-2010. Red and blue lines indicate average trends calculated using SFI2 data or SFI3 data, respectively. Black lines indicate average trends obtained after combining predictions for both forest inventories. Trends for individual forest plots are shown in light grey. Change mean and s.d. – Mean and standard deviation of the magnitude of change in NDD, according to the Theil-Sen approach. Incr./Decr. – Percentage of plots (among those where the species is present) with significant increase/decrease ($P < 0.05$) in NDD, according to the Mann-Kendall trend test. Corr. SPEI – Pearson correlation between the slope of NDD and the slope of the Standardized Precipitation-Evapotranspiration Index (scale = 12 months).

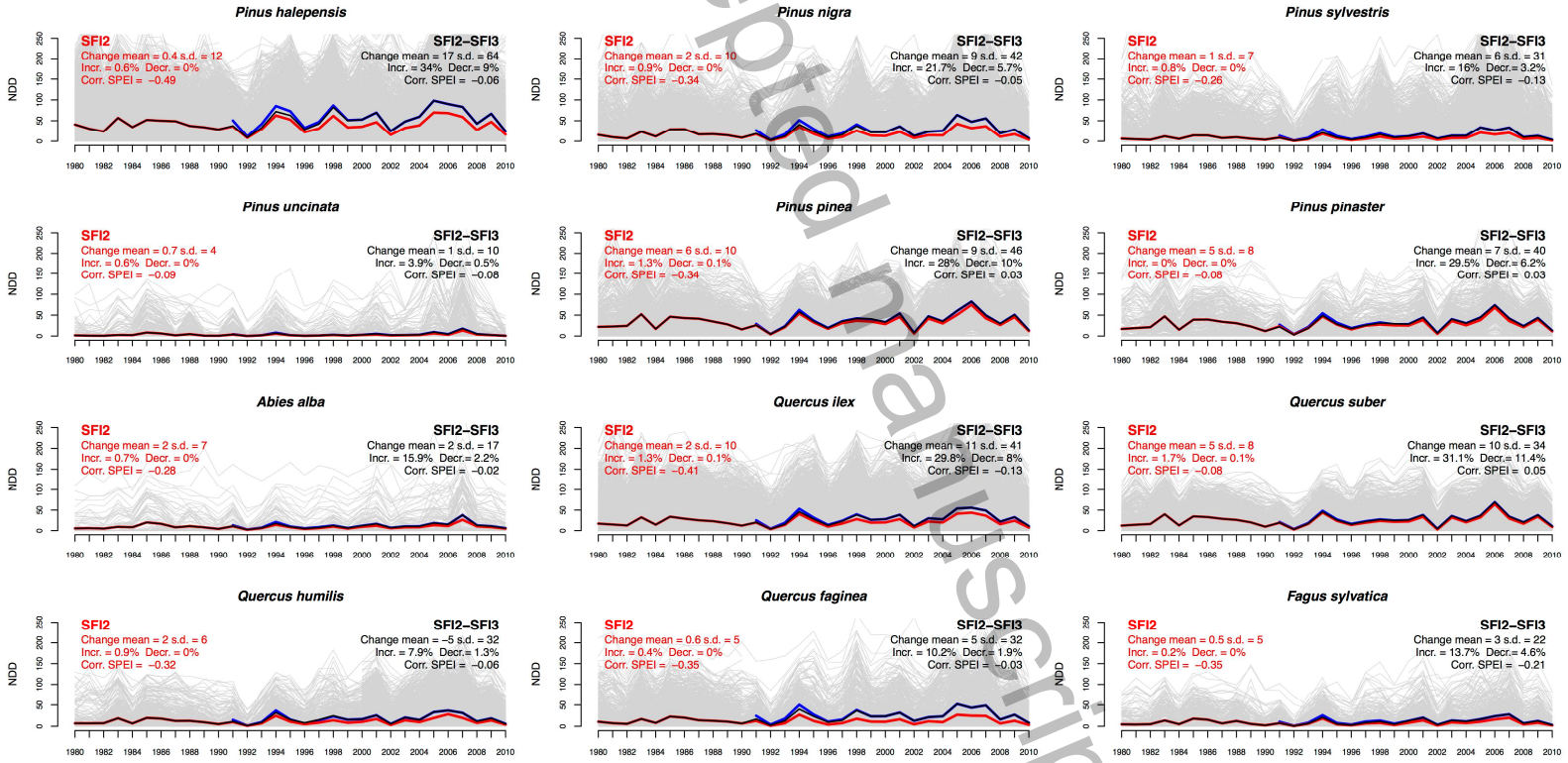

4. Discussion

4.1 Recent trends of drought stress in Catalonia

Our model predicted an increase in intensity and duration of drought stress for most tree species in Catalonia, but we found that changes in drought stress mostly originated from changes in leaf area rather than from climatic aridification. Since the mid twentieth century, forest cover in the northwest Mediterranean Basin is increasing due to the progressive colonization of former agricultural areas and the densification of pre-existing forests associated to the decrease of forest management activities (Améztegui et al., 2010; Weissteiner et al., 2011). One of the consequences of this fuel accumulation is the increased frequency of large wildfires (Pausas, 2004; Pausas & Fernández-Muñoz, 2012); the largest ones in Catalonia occurred between the two SFI inventories (Díaz-Delgado et al., 2004). The footprint of those events is clear in the spatial distribution of LAI changes, but does not compensate for the increase in LAI over most of the region (Fig. 3). Mortality rates in the Iberian Peninsula have been associated to forest densification in dry sites (Vilà-Cabrera et al., 2011; Vayreda et al., 2012; Ruiz-Benito et al., 2013). Our results support the idea that increasing forest management could reverse the observed general increase in drought stress, regardless of the observed increase in temperatures (Cotillas et al., 2009). This would, in turn, lower fire risk as fires in the study area are partially controlled by fuel (Pausas & Fernández-Muñoz, 2012; Pausas & Paula, 2012).

On average, Mediterranean tree species were predicted to experience higher intensity and duration of drought stress than sub-Mediterranean or temperate species. These results do not imply that Mediterranean plants are more likely to exhibit drought stress effects, because their ability to tolerate stress is much higher. Choat et al. (2012) recently showed that many tree species operate with narrow hydraulic safety margins against injurious levels of drought

577 stress and that these safety margins are unrelated to rainfall regimes at global scale. This view
578 is also supported by recent observations of crown defoliation not being restricted to the most
579 drought-sensitive species but affecting all tree species examined (Carnicer et al., 2011). If we
580 neglect intraspecific variation in drought resistance, one should expect larger drought-related
581 effects for a given species in those stands where climatic, soil and vegetation conditions lead
582 to unusually high stress values with respect to those found across the distribution of the
583 species (see Figs. S4.4 and S4.6 in Appendix S4). For example, the 151 days of drought stress
584 for *P. sylvestris* in the *Prades* validation stand, where high mortality rates have been observed
585 since the 1990s (Martínez-Vilalta & Piñol, 2002; Poyatos et al., 2013), corresponds to 99.7%
586 in the cumulative distribution of NDD for this species in Catalonia.

587 *4.2 Potential applications*

588 We have shown that running a process-based model on forest inventory plots can be used to
589 obtain species-specific estimates of drought stress at landscape and regional scales. This
590 approach could be adopted to identify areas where the combination of forest structure, species
591 composition, soil conditions and current climate makes them highly vulnerable to drought
592 impacts. In addition, when coupled with daily meteorological data (and assuming repeated
593 forest inventory surveys), this approach could be used to routinely monitor plant drought
594 stress over large areas, complementing remote sensing indices that are normally used to
595 monitor the effects of drought stress (Deshayes et al., 2006). Using daily meteorological data
596 would avoid the need to conduct temporal downscaling, which in our case involved many
597 assumptions such as the lack of correlation between temperature and precipitation. Compared
598 to hydrological models that already provide soil moisture estimates in agricultural drought
599 monitoring (e.g., Sepulcre-Canto et al., 2012; Sheffield and Wood, 2008), our approach
600 would provide species-specific drought stress estimates for forest systems. Finally, combining
601 remote sensing technologies, such as LiDAR or multispectral imaging, with field data could

602 be used to obtain spatially continuous information about forest structure (Holopainen and
603 Kalliovirta, 2006; Estornell et al., 2011) and, hence, to generate drought stress predictions for
604 stands not included in forest inventory plots.

605 Before promoting it for practical use to monitor drought stress at the regional scale,
606 however, our model should be further validated by comparison of observed soil moisture and
607 water fluxes in a larger number of stands spread over the region. Other regional-level
608 validation exercises (e.g., the comparison between predicted stress and observed drought
609 impacts or the comparison of modeled exported water with stream flow data) may be
610 necessary but difficult to conduct due to the influence of additional processes (e.g., drought-
611 related mortality or lateral water transfer) not currently implemented in the model.

612 *4.3 Accuracy and temporal variation of LAI estimates*

613 Modeling transpiration rates accurately is crucial for predicting soil moisture and drought
614 stress variations; and transpiration rates primarily depend on LAI. In similar studies
615 addressing drought stress patterns at the regional scale, Ruffault et al. (2013) relied on model-
616 optimized LAI estimates, while Chakroun et al. (2014) used the relationship between field
617 LAI values and remote sensing vegetation indices. In contrast with these studies, we
618 estimated species-specific LAI values from forest inventory data using relationships between
619 LAI and basal area (Table S2.1). While this approach can be more precise than using satellite-
620 derived estimates, some biases may remain because the relationship between LAI and basal
621 area is influenced by factors such as forest management (e.g., Davi et al., 2008; Le Dantec et
622 al., 2000). Another limitation of using forest inventory data for LAI estimation is that LAI
623 values are assumed to remain constant when computing drought stress before or after the year
624 of survey. We found that the accuracy of our stand-level estimates was strongly dependent on
625 this temporal extrapolation, although regional-level averages were much less sensitive (Fig.
626 5). Even if we exclude LAI changes derived from major changes in vegetation structure (e.g.,

627 forest encroachment, fire or human-mediated disturbances), plants are known to adjust their
628 leaf area to cope with variations in drought stress (e.g., Le Dantec et al., 2000; Limousin et
629 al., 2009; Maseda & Fernández, 2006). Accounting for drought-related LAI changes would
630 require coupling water balance with carbon balance in the same model (e.g., Hoff & Rambal,
631 2003). Alternatively, combining forest inventory with remotely sensed data would allow
632 tracking LAI variations caused by this or other processes (e.g., Chakroun et al., 2014).

633 *4.4 Availability of belowground data*

634 Availability of good quality belowground data is also important to increase the usefulness of
635 our approach, because of the strong dependency of the water balance on rooting depth and
636 soil characteristics like depth, texture or stoniness. Our results indicate that substantial biases
637 in drought stress may occur when the depth of shallow soils (< 50 cm) is overestimated.
638 Ideally, soil attributes of forest plots should be obtained from forest inventory or other field
639 surveys. Alternatively, spatial variation in soil attributes may be modeled from topographic,
640 lithological and land use information (Boer et al., 1996; Zheng et al., 1996; Tesfa et al.,
641 2009). Regarding root systems, solving for an optimized root distribution on the basis of
642 environmental conditions produces estimates that may not be realistic, depending on the
643 model definition. For example, our model did not include any penalization derived from the
644 energetic costs of creating and maintaining roots (Schymanski et al., 2008). Moreover,
645 slightly different root distributions would have been obtained if we had chosen to minimize
646 drought stress or maximize net primary production, instead of maximizing transpiration
647 (Collins and Bras, 2007; Kleidon and Heimann, 1998). Given the difficulty to obtain root
648 profiles in the field for even a moderate number of forest stands, we think that the strategy of
649 optimizing root distributions provides an operational solution. An additional modeling issue
650 arises because deep roots frequently occurs within rock fissures and cracks in sclerophyllous
651 vegetation (Canadell et al., 1996; Keeley et al., 2012). Accounting for such additional soil

652 water capacity may be important when modeling transpiration and drought stress in areas with
653 shallow soils (Rambal et al., 2003; Ruffault et al., 2013), as we did the *Prades* site (in
654 agreement with Barbeta et al., 2014).

655 *4.5 Limitations of the current model design*

656 In this study we opted for a process-based model where – compared to ecosystem models,
657 land surface models or dynamic global vegetation models – many processes were highly
658 condensed and others were simply absent. While this strategy facilitated calibration over the
659 study area and provided satisfactory validation results, additional processes may need to be
660 considered. We mentioned above that considering carbon balance would allow addressing
661 temporal changes in LAI. Predictions of drought stress would likely be more accurate if the
662 model included the down-regulation of stomata conductance derived from increased CO_2
663 concentrations (e.g., Dufrêne et al., 2005; Keenan et al., 2011). Distinguishing between plant
664 cohorts in our model required splitting the maximum stand transpiration, calculated following
665 Granier (1999), among them. Experimental data would be necessary to calibrate species-
666 specific relationships between LAI and maximum transpiration. The use of a radiation
667 transfer module including other wavelengths than visible could provide a better estimation of
668 the evapotranspiration fraction assigned to the understory (Balandier et al., 2006).
669 Furthermore, whole-plant conductance was assumed to be independent of previous drought
670 events (i.e., hysteresis was lacking in the relationship between soil water potential and plant
671 conductance) (Limousin et al., 2009; Sus et al., 2014). Although seldom considered, hydraulic
672 redistribution may buffer the effects of changes in soil moisture regimes and thereby increase
673 the resilience of ecosystems to changes in patterns of precipitation (Horton and Hart, 1998;
674 Weltzin et al., 2003). Finally, a one-dimensional (vertical) model like ours may inaccurately
675 predict soil moisture dynamics when non-local controls (i.e. lateral transport by subsurface or
676 overland flow) dominate (Grayson and Western, 1997). Incorporating lateral water transfer

could have potentially lowered the amount of drought stress for some plots. However, in Mediterranean areas evapotranspiration exceeds precipitation during long periods and vertical fluxes dominate under these conditions (Garcia-Estringana et al., 2013; Grayson and Western, 1997).

4.6 From drought stress to drought impacts

Predicting drought-related events of tree decline or mortality resulting from expected climatic changes requires to effectively link drought stress estimates to drought-related effects. Predicting drought impacts is hampered by our incomplete knowledge on how drought stress changes demographic rates. For example, different species and life stages may respond to drought stress measured at different temporal scales (Pasho et al., 2011). Furthermore, drought-induced mortality can be in fact the result of drought stress interacting with other factors like pests and pathogens (McDowell et al., 2011; Oliva et al., 2014), which may explain why attempts to predict the occurrence of mortality have been generally unsuccessful (McDowell et al., 2013). Physiological models can relate climatic variability with drought-related mortality at the individual and stand levels (e.g., Martinez-Vilalta et al., 2002; Zavala & Bravo de la Parra, 2005; Tague et al., 2013), but their predictive capacity remains to be tested at larger scales. Dynamic global vegetation models, gap models or landscape dynamics models may be useful to study drought impacts on vegetation structure and composition over large areas (e.g., Bugmann and Cramer 1998; Fyllas and Troumbis, 2009; Gustafson & Sturtevant, 2013; Mouillot et al., 2001), but further modeling efforts are needed to strengthen the link between predicted drought stress and actual demographic rates before they can be used to accurately predict drought impacts (Keane et al., 2001).

Acknowledgements

This study has received financial support from the projects CGL2011-29539, CGL2010-16373, CGL2012-39938-C02-01, CGL2013-46808-R and MONTES-Consolider CSD2008-00040 granted by the Spanish Ministry of Education and Science (MEC). This is a contribution to the ERA-NET INFORMED project. Additional support to M.D.C came from research contract granted by the Spanish Ministry of Economy and Competitiveness (RYC-2012-11109). We thank Miquel Ninyerola and Meritxell Batalla (Botany Department, Autonomous University of Barcelona) for generating spatially explicit climatic predictions from data provided by the Spanish Meteorological Agency and the Spanish Ministry of Marine and Rural Environment; and Jaume Fons (Geography Department, Autonomous University of Barcelona) for generating soil depth estimates. We also thank Assu Gil and Mario Beltrán (CTFC) for useful discussions and technical assistance.

Bibliography

Allen, C.D., Macalady, A.K., Chenchouni, H., Bachelet, D., McDowell, N., Vennetier, M., Kitzberger, T., Rigling, A., Breshears, D.D., Hogg, E.H. (Ted), Gonzalez, P., Fensham, R., Zhang, Z., Castro, J., Demidova, N., Lim, J.-H., Allard, G., Running, S.W., Semerci, A., Cobb, N., 2010. A global overview of drought and heat-induced tree mortality reveals emerging climate change risks for forests. For. Ecol. Manage. 259, 660–684. doi:10.1016/j.foreco.2009.09.001

Améztegui, A., Brotons, L., Coll, L., 2010. Land-use changes as major drivers of mountain pine (Pinus uncinata Ram.) expansion in the Pyrenees. Glob. Ecol. Biogeogr. 19, 632–641. doi:10.1111/j.1466-8238.2010.00550.x

Aubin, I., Beaudet, M., Messier, C., 2000. Light extinction coefficients specific to the understory vegetation of the southern boreal forest, Quebec. Can. J. For. Res. 30, 168–177. doi:10.1139/x99-185

Balandier, P., Sonohat, G., Sinoquet, H., Varlet-Grancher, C., Dumas, Y., 2006. Characterisation, prediction and relationships between different wavebands of solar radiation transmitted in the understory of even-aged oak (*Quercus petraea*, *Q. robur*) stands. Trees 20, 363–370.

Barbeta, A., Mejía-Chang, M., Ogaya, R., Voltas, J., Dawson, T.E., Peñuelas, J., 2014. The combined effects of a long-term experimental drought and an extreme drought on the use of plant-water sources in a Mediterranean forest. Glob. Chang. Biol. doi:10.1111/gcb.12785

Bartlett, M.K., Scoffoni, C., Sack, L., 2012. The determinants of leaf turgor loss point and prediction of drought tolerance of species and biomes: a global meta-analysis. Ecol. Lett. 15, 393–405. doi:10.1111/j.1461-0248.2012.01751.x

735 Beguería, S., Vicente-Serrano, S.M., 2013. SPEI: Calculation of the Standardised
736 Precipitation-Evapotranspiration Index. R package version 1.6. http://CRAN.R-
737 project.org/package=SPEI
738 Boer, M., Barrio, G. Del, Puigdefábregas, J., 1996. Mapping soil depth classes in dry
739 Mediterranean areas using terrain attributes derived from a digital elevation model.
740 Geoderma 72, 99–118.
741 Boughton, W., 1989. A review of the USDA SCS curve number method. Aust. J. Soil Res.
742 27, 511–523.
743 Bréda, N.J.J., 2003. Ground-based measurements of leaf area index: a review of methods,
744 instruments and current controversies. J. Exp. Bot. 54, 2403–17. doi:10.1093/jxb/erg263
745 Bugmann, H., Cramer, W., 1998. Improving the behaviour of forest gap models along
746 drought gradients. For. Ecol. Manage. 103, 247–263.
747 Burriel, J.A., Gracia, C., Ibàñez, J.J., Mata, T., Vayreda, J., 2004. Inventari Ecològic i
748 Forestal de Catalunya, 10 volumes. CREAF, Bellaterra, Spain.
749 Canadell, J., Jackson, R., Ehleringer, J., Mooney, H., Sala, O., Schulze, E., 1996. Maximum
750 rooting depth of vegetation types at the global scale. Oecologia 108, 583–595.
751 doi:10.1007/BF00329030
752 Carnicer, J., Coll, M., Ninyerola, M., Pons, X., Sánchez, G., Peñuelas, J., 2011. Widespread
753 crown condition decline, food web disruption, and amplified tree mortality with
754 increased climate change-type drought. Proc. Natl. Acad. Sci. U. S. A. 108, 1474–8.
755 doi:10.1073/pnas.1010070108
756 Casper, B., Jackson, R., 1997. Plant competition underground. Annu. Rev. Ecol. Syst. 28,
757 545–570.
758 Chakroun, H., Mouillot, F., Nasr, Z., Nouri, M., Ennajah, a. & Ourcival, J.M., 2014.
759 Performance of LAI-MODIS and the influence on drought simulation in a Mediterranean
760 forest. Ecohydrology 7, 1014–1028.
761 Choat, B., Jansen, S., Brodribb, T.J., Cochard, H., Delzon, S., Bhaskar, R., Bucci, S.J., Feild,
762 T.S., Gleason, S.M., Hacke, U.G., Jacobsen, A.L., Lens, F., Maherali, H., Martínez-
763 Vilalta, J., Mayr, S., Mencuccini, M., Mitchell, P.J., Nardini, A., Pittermann, J., Pratt,
764 R.B., Sperry, J.S., Westoby, M., Wright, I.J., Zanne, A.E., 2012. Global convergence in
765 the vulnerability of forests to drought. Nature 491, 752–755. doi:10.1038/nature11688
766 Collins, D.B.G., Bras, R.L., 2007. Plant rooting strategies in water-limited ecosystems. Water
767 Resour. Res. 43, W06407. doi:10.1029/2006WR005541
768 Cotillas, M., Sabaté, S., Gracia, C., Espelta, J.M., 2009. Growth response of mixed
769 mediterranean oak coppices to rainfall reduction. Could selective thinning have any
770 influence on it? For. Ecol. Manage. 258, 1677–1683. doi:10.1016/j.foreco.2009.07.033
771 CREAF/UPC/ETC/IRTA, 2011. Adaptacions al Canvi Climàtic en l'Ús de l'Aigua.
772 Dai, A., 2011. Drought under global warming: a review. Wiley Interdiscip. Rev. Clim. Chang.
773 2, 45–65. doi:10.1002/wcc.81
774 Davi, H., Baret, F., Huc, R., Dufrêne, E., 2008. Effect of thinning on LAI variance in
775 heterogeneous forests. For. Ecol. Manage. 256, 890–899.
776 doi:10.1016/j.foreco.2008.05.047
777 Davi, H., Dufrêne, E., Granier, A., Le Dantec, V., Barbaroux, C., François, C., Bréda, N.,
778 2005. Modelling carbon and water cycles in a beech forest Part II.: Validation of the
779 main processes from organ to stand scale. Ecol. Modell. 185, 387–405.
780 doi:10.1016/j.ecolmodel.2005.01.003
781 Delzon, S., Cochard, H., 2014. Recent advances in tree hydraulics highlight the ecological
782 significance of the hydraulic safety margin. New Phytol. 203, 355–358.
783 doi:10.1111/nph.12798

784 Deshayes, M., Guyon, D., Jeanjean, H., Stach, N., Jolly, A., Hagolle, O., 2006. The
785 contribution of remote sensing to the assessment of drought effects in forest ecosystems.
786 Ann. For. Sci. 63, 579–595.
787 Díaz-Delgado, R., Lloret, F., Pons, X., 2004. Spatial patterns of fire occurrence in Catalonia,
788 NE, Spain. Landsc. Ecol. 19, 731–745. doi:10.1007/s10980-005-0183-1
789 Dufrêne, E., Davi, H., François, C., Maire, G. Le, Dantec, V. Le, Granier, A., 2005.
790 Modelling carbon and water cycles in a beech forest Part I: Model description and
791 uncertainty analysis on modelled NEE. Ecol. Modell. 185, 407–436.
792 doi:10.1016/j.ecolmodel.2005.01.004
793 Estornell, J., Ruiz, L., Velázquez-Marti, B., 2011. Study of shrub cover and height using
794 LIDAR data in a Mediterranean area. For. Sci. 57, 171–179.
795 FAO/IIASA/ISRIC/ISS-CAS/JRC 2009. Harmonized World Soil Database (version 1.1).
796 FAO, Rome, Italy and IIASA, Laxenburg, Austria.
797 Fyllas, N.M., Troumbis, A.Y., 2009. Simulating vegetation shifts in north-eastern
798 Mediterranean mountain forests under climatic change scenarios. Glob. Ecol. Biogeogr.
799 18, 64–77. doi:10.1111/j.1466-8238.2008.00419.x
800 Garcia-Estringana, P., Latron, J., Llorens, P., Gallart, F., 2013. Spatial and temporal dynamics
801 of soil moisture in a Mediterranean mountain area (Vallcebre , NE Spain). Ecohydrology
802 753, 741–753. doi:10.1002/eco.1295
803 Gash, J., Lloyd, C., Lachaud, G., 1995. Estimating sparse forest rainfall interception with an
804 analytical model. J. Hydrol. 170.
805 Gao, B.C., 1996. NDWI - A normalized difference water index for remote sensing of
806 vegetation liquid water from space. Remote Sens. Environ. 58, 257–266.
807 doi:10.1016/S0034-4257(96)00067-3
808 Gobron, N., Pinty, B., Taberner, M., Mélin, F., Verstraete, M.M., Widlowski, J.L., 2006.
809 Monitoring the photosynthetic activity of vegetation from remote sensing data. Adv. Sp.
810 Res. 38, 2196–2202. doi:10.1016/j.asr.2003.07.079
811 Granier, A., Bréda, N., Biron, P., Villette, S., 1999. A lumped water balance model to
812 evaluate duration and intensity of drought constraints in forest stands. Ecol. Modell. 116,
813 269–283.
814 Granier, A., Reichstein, M., Bréda, N., Janssens, I.A., Falge, E., Ciais, P., Grünwald, T.,
815 Aubinet, M., Berbigier, P., Bernhofer, C., Buchmann, N., Facini, O., Grassi, G.,
816 Heinesch, B., Ilvesniemi, H., Keronen, P., Knohl, A., Köstner, B., Lagergren, F.,
817 Lindroth, A., Longdoz, B., Loustau, D., Mateus, J., Montagnani, L., Nys, C., Moors, E.,
818 Papale, D., Peiffer, M., Pilegaard, K., Pita, G., Pumpanen, J., Rambal, S., Rebmann, C.,
819 Rodrigues, A., Seufert, G., Tenhunen, J., Vesala, T., Wang, Q., 2007. Evidence for soil
820 water control on carbon and water dynamics in European forests during the extremely
821 dry year: 2003. Agric. For. Meteorol. 143, 123–145.
822 doi:10.1016/j.agrformet.2006.12.004
823 Grayson, R., Western, A., 1997. Preferred states in spatial soil moisture patterns: Local and
824 nonlocal controls. Water Resour. Res. 33, 2897–2908.
825 Gustafson, E.J., Sturtevant, B.R., 2013. Modeling forest mortality caused by drought stress:
826 Implications for climate change. Ecosystems 16, 60–74. doi:10.1007/s10021-012-9596-1
827 Heim, R.R., 2002. Century drought indices used in the United States. Bull. Am. Meteorol.
828 Soc. 1149–1165.
829 Hoff, C., Rambal, S., 2003. An examination of the interaction between climate, soil and leaf
830 area index in a *Quercus ilex* ecosystem. Ann. For. Sci. 60, 153–161. doi:10.1051/forest
831 Holopainen, M., Kalliovirta, J., 2006. Modern data adquisition for forest inventories, in:
832 Kangas, A., Maltamo, M. (Eds.), Forest Inventory - Methodology and Applications.
833 Springer, Netherlands, pp. 343–362.

834 Horton, J., Hart, S., 1998. Hydraulic lift: a potentially important ecosystem process. Trends
835 Ecol. Evol. 13, 232–235.
836 Jarvis, P., McNaughton, K., 1986. Stomatal control of transpiration: Scaling Up from leaf to
837 region. Adv. Ecol. Res. 15, 1–49.
838 Joffre, R., Rambal, S., 1993. How tree cover influences the water balance of Mediterranean
839 rangelands. Ecology 74, 570–582.
840 Keane, R., Austin, M., Field, C., Huth, A., 2001. Tree mortality in gap models: Application to
841 climate change. Clim. Change 51, 509–540.
842 Keeley, J.E., Bond, W.J., Bradstock, R.A., Pausas, J.G., Rundel, P.W., 2012. Fire in
843 Mediterranean Ecosystems. Cambridge University Press, New York.
844 Keenan, T., Maria Serra, J., Lloret, F., Ninyerola, M., Sabate, S., 2011. Predicting the future
845 of forests in the Mediterranean under climate change, with niche- and process-based
846 models: CO2 matters! Glob. Chang. Biol. 17, 565–579. doi:10.1111/j.1365-
847 2486.2010.02254.x
848 Kerr, Y.H., Waldteufel, P., Richaume, P., Wigneron, J.P., Ferrazzoli, P., Mahmoodi, A.,
849 Bitar, A. Al, Cabot, F., Gruhier, C., Juglea, S.E., Leroux, D., Mialon, A., Delwart, S.,
850 2012. The SMOS Soil Moisture Retrieval Algorithm. Geosci. Remote Sens. 50, 1384–
851 1403.
852 Kleidon, A., Heimann, M., 1998. A method of determining rooting depth from a terrestrial
853 biosphere model and its impacts on the global water and carbon cycle. Glob. Chang.
854 Biol. 4, 275–286. doi:10.1046/j.1365-2486.1998.00152.x
855 Klein, T., 2014. The variability of stomatal sensitivity to leaf water potential across tree
856 species indicates a continuum between isohydric and anisohydric behaviours. Funct.
857 Ecol. 28, 1313–1320. doi:10.1111/1365-2435.12289
858 Kogan, F.N., 1997. Global drought watch from space. Bull. Am. Meteorol. Soc. 78, 621–636.
859 Latron, J., Llorens, P., Soler, M., Poyatos, R., Rubio, C., Muzylo, A., Martínez-Carreras, N.
860 Delgado, J., Regüés, D., Catari, G., Nord, G., Gallart, F., 2010. Hydrology in a
861 Mediterranean mountain environment-The Vallcebre research basins (North Eastern
862 Spain). I. 20 years of investigations of hydrological dynamics. IAHS Publ. 336, 38–43.
863 Lafont, S., Zhao, Y., Calvet, J.C., Peylin, P., Ciais, P., Maignan, F., Weiss, M., 2012.
864 Modelling LAI, surface water and carbon fluxes at high-resolution over France:
865 Comparison of ISBA-A-gs and ORCHIDEE. Biogeosciences 9, 439–456.
866 doi:10.5194/bg-9-439-2012
867 Lindner, M., Maroschek, M., Netherer, S., Kremer, A., Barbati, A., Garcia-Gonzalo, J., Seidl,
868 R., Delzon, S., Corona, P., Kolström, M., Lexer, M.J., Marchetti, M., 2010. Climate
869 change impacts, adaptive capacity, and vulnerability of European forest ecosystems. For.
870 Ecol. Manage. 259, 698–709. doi:10.1016/j.foreco.2009.09.023
871 Le Dantec, V., Dufrêne, E., Saugier, B., 2000. Interannual and spatial variation in maximum
872 leaf area index of temperate deciduous stands. For. Ecol. Manage. 134, 71–81.
873 doi:10.1016/S0378-1127(99)00246-7
874 Le Maire, G., Davi, H., Soudani, K., François, C., Le Dantec, V., Dufrêne, E., 2005.
875 Modeling annual production and carbon fluxes of a large managed temperate forest using
876 forest inventories, satellite data and field measurements. Tree Physiol. 25, 859–872.
877 Limousin, J.M., Rambal, S., Ourcival, J.M., Rocheteau, A., Joffre, R., Rodriguez-Cortina, R.,
878 2009. Long-term transpiration change with rainfall decline in a Mediterranean *Quercus*
879 *ilex* forest. Glob. Chang. Biol. 15, 2163–2175. doi:10.1111/j.1365-2486.2009.01852.x
880 Lischke, H., Zimmermann, N.E., Bolliger, J., Rickebusch, S., Löffler, T.J., 2006. TreeMig: A
881 forest-landscape model for simulating spatio-temporal patterns from stand to landscape
882 scale. Ecol. Modell. 199, 409–420. doi:10.1016/j.ecolmodel.2005.11.046
883 Mann, H., 1945. Nonparametric tests against trend. Econometrica 13, 245–259.

884 Martínez-Vilalta, J., Piñol, J., 2002. Drought-induced mortality and hydraulic architecture in
885 pine populations of the NE Iberian Peninsula. For. Ecol. Manage. 161, 247–256.
886 Martinez-Vilalta, J., Piñol, J., Beven, K., 2002. A hydraulic model to predict drought-induced
887 mortality in woody plants: an application to climate change in the Mediterranean. Ecol.
888 Modell. 155, 127–147.
889 Martínez-Vilalta, J., Poyatos, R., Aguadé, D., Retana, J., Mencuccini, M., 2014. A new look
890 at water transport regulation in plants. New Phytol. doi:10.1111/nph.12912
891 Maseda, P.H., Fernández, R.J., 2006. Stay wet or else: three ways in which plants can adjust
892 hydraulically to their environment. J. Exp. Bot. 57, 3963–77. doi:10.1093/jxb/erl127
893 McDowell, N., Fisher, R., Xu, C., Domec, J., Hölttä, T., Mackay, D., Sperry, J.S., Boutz, A.,
894 Dickman, L., Gehres, N., Limousin, J.-M., Macalady, A., Martínez-Vilalta, J.,
895 Mencuccini, M., Plaut, J.A., Ogée, J., Pangle, R., Rasse, D., Ryan, M., Sevanto, S.,
896 Waring, R., Williams, A., Yepez, E., Pockman, W.T., 2013. Evaluating theories of
897 drought-induced vegetation mortality using a multimodel–experiment framework. New
898 Phytol. 200, 304–321.
899 McDowell, N., Pockman, W.T., Allen, C.D., Breshears, D.D., Cobb, N., Kolb, T., Plaut, J.,
900 Sperry, J., West, A., Williams, D.G., Yepez, E. A., 2008. Mechanisms of plant survival
901 and mortality during drought: why do some plants survive while others succumb to
902 drought? New Phytol. 178, 719–39. doi:10.1111/j.1469-8137.2008.02436.x
903 McDowell, N.G., Beerling, D.J., Breshears, D.D., Fisher, R.A., Raffa, K.F., Stitt, M., 2011.
904 The interdependence of mechanisms underlying climate-driven vegetation mortality.
905 Trends Ecol. Evol. 26, 523–32. doi:10.1016/j.tree.2011.06.003
906 McKee, T., Doesken, N., Kleist, J., 1993. The relationship of drought frequency and duration
907 to time scales, in: Eighth Conference on Applied Climatology. pp. 17–22.
908 Miralles, D.G., Gash, J.H., Holmes, T.R.H., de Jeu, R.A.M., Dolman, A.J., 2010. Global
909 canopy interception from satellite observations. J. Geophys. Res. 115, D16122.
910 doi:10.1029/2009JD013530
911 Mouillot, F., Rambal, S., Joffre, R., 2002. Simulating climate change impacts on fire
912 frequency and vegetation dynamics in a Mediterranean-type ecosystem. Glob. Chang.
913 Biol. 8, 423–437.
914 Mouillot, F., Rambal, S., Lavorel, S., 2001. A generic process-based SImulator for
915 meditERRanean landscApes (SIERRA): design and validation exercises. For. Ecol.
916 Manage. 147, 75–97. doi:10.1016/S0378-1127(00)00432-1
917 Ninyerola, M., Pons, X., Roure, J.M., 2000. A methodological approach of climatological
918 modelling of air temperature and precipitation through GIS techniques. Int. J. Climatol.
919 20, 1823–1841.
920 Oliva, J., Stenlid, J., Martínez□Vilalta, J., 2014. The effect of fungal pathogens on the water
921 and carbon economy of trees: implications for drought-induced mortality. New Phytol.
922 Pasho, E., Camarero, J.J., de Luis, M., Vicente-Serrano, S.M., 2011. Impacts of drought at
923 different time scales on forest growth across a wide climatic gradient in north-eastern
924 Spain. Agric. For. Meteorol. 151, 1800–1811. doi:10.1016/j.agrformet.2011.07.018
925 Palmer, W., 1965. Meteorological Drought. Research Papers 45.
926 Pausas, J.G., 2004. Changes in Fire and Climate in the Eastern Iberian Peninsula
927 (Mediterranean Basin). Clim. Change 63, 337–350.
928 Pausas, J.G., Fernández-Muñoz, S., 2012. Fire regime changes in the Western Mediterranean
929 Basin: from fuel-limited to drought-driven fire regime. Clim. Change 110, 215–226.
930 doi:10.1007/s10584-011-0060-6
931 Pausas, J.G., Paula, S., 2012. Fuel shapes the fire-climate relationship: evidence from
932 Mediterranean ecosystems. Glob. Ecol. Biogeogr. 21, 1074–1082.

933 Pons, X., Ninyerola, M., 2008. Mapping a topographic global solar radiation model
934 implemented in a GIS and refined with ground data. Int. J. Climatol. 1834, 1821–1834.
935 doi:10.1002/joc
936 Poyatos, R., Aguadé, D., Galiano, L., Mencuccini, M., Martínez-Vilalta, J., 2013. Drought-
937 induced defoliation and long periods of near-zero gas exchange play a key role in
938 accentuating metabolic decline of Scots pine. New Phytol. 200, 388–401.
939 Poyatos, R., Llorens, P., Gallart, F., 2005. Transpiration of montane Pinus sylvestris L. and
940 *Quercus pubescens* Willd. forest stands measured with sap flow sensors in NE Spain.
941 Hydrol. Earth Syst. Sci. Discuss. 2, 1011–1046. doi:10.5194/hessd-2-1011-2005
942 Poyatos, R., Villagarcía, L., Domingo, F., Piñol, J., Llorens, P., 2007. Modelling
943 evapotranspiration in a Scots pine stand under Mediterranean mountain climate using the
944 GLUE methodology. Agric. For. Meteorol. 146, 13–28.
945 doi:10.1016/j.agrformet.2007.05.003
946 Prentice, I.C., Sykes, M.T., Cramer, W., 1993. A simulation model for the transient effects of
947 climate change on forest landscapes. Ecol. Modell. 65, 51–70. doi:10.1016/0304-
948 3800(93)90126-D
949 Rambal, S., Ourcival, J.M., Joffre, R., Mouillot, F., Nouvellon, Y., Reichstein, M.,
950 Rocheteau, A., 2003. Drought controls over conductance and assimilation of a
951 Mediterranean evergreen ecosystem: Scaling from leaf to canopy. Glob. Chang. Biol. 9,
952 1813–1824. doi:10.1111/j.1365-2486.2003.00687.x
953 Ritchie, J., 1972. Model for predicting evaporation from a row crop with incomplete cover.
954 Water Resour. Res. 8, 1204–1213.
955 Ruffault, J., Martin-StPaul, N.K., Duffet, C., Goge, F., Mouillot, F., 2014. Projecting future
956 drought in Mediterranean forests: bias correction of climate models matters! Theor.
957 Appl. Climatol. 117, 113–122. doi:10.1007/s00704-013-0992-z
958 Ruffault, J., Martin-StPaul, N.K., Rambal, S., Mouillot, F., 2013. Differential regional
959 responses in drought length, intensity and timing to recent climate changes in a
960 Mediterranean forested ecosystem. Clim. Change 117, 103–117. doi:10.1007/s10584-
961 012-0559-5
962 Ruiz-Benito, P., Lines, E.R., Gómez-Aparicio, L., Zavala, M.A., Coomes, D.A., 2013.
963 Patterns and drivers of tree mortality in iberian forests: climatic effects are modified by
964 competition. PLoS One 8, e56843. doi:10.1371/journal.pone.0056843
965 Running, S., Coughlan, J., 1988. A general model of forest ecosystem processes for regional
966 applications. I. Hydrologic balance, canopy gas exchange and primary production
967 processes. Ecol. Modell. 42, 125–154.
968 Saxton, K.E., Rawls, W.J., Romberger, J.S., Papendick, R.I., 1986. Estimating generalized
969 soil-water characteristics from texture. Soil Sci. Soc. Am. J. 50, 1031–1036.
970 Schenk, H., Jackson, R., 2002. The global biogeography of roots. Ecol. Monogr. 72, 311–328.
971 Schymanski, S.J., Sivapalan, M., Roderick, M.L., Beringer, J., Hutley, L.B., 2008. An
972 optimality-based model of the coupled soil moisture and root dynamics. Hydrol. Earth
973 Syst. Sci. 12, 913–932. doi:10.5194/hess-12-913-2008
974 Sen, P., 1968. Estimates of the regression coefficient based on Kendall's tau. J. Am. Stat.
975 Assoc. 63, 1379–1389.
976 Sepulcre-Canto, G., Horion, S., Singleton, A., Carrao, H., Vogt, J., 2012. Development of a
977 Combined Drought Indicator to detect agricultural drought in Europe. Nat. Hazards
978 Earth Syst. Sci. 12, 3519–3531. doi:10.5194/nhess-12-3519-2012
979 Sheffield, J., Wood, E.F., 2008. Global Trends and Variability in Soil Moisture and Drought
980 Characteristics, 1950–2000, from Observation-Driven Simulations of the Terrestrial
981 Hydrologic Cycle. J. Clim. 21, 432–458. doi:10.1175/2007JCLI1822.1

Sitch, S., Smith, B., Prentice, I.C., Arneth, a., Bondeau, a., Cramer, W., Kaplan, J.O., Levis, S., Lucht, W., Sykes, M.T., Thonicke, K., Venevsky, S., 2003. Evaluation of ecosystem dynamics, plant geography and terrestrial carbon cycling in the LPJ dynamic global vegetation model. Glob. Chang. Biol. 9, 161–185. doi:10.1046/j.1365-2486.2003.00569.x

Sperry, J.S., Adler, F.R., Campbell, G.S., Comstock, J.P., 1998. Limitation of plant water use by rhizosphere and xylem conductance: results from a model. Plant. Cell Environ. 21, 347–359.

Stolf, R., Thurler, Á., Oliveira, O., Bacchi, S., Reichardt, K., 2011. Method to estimate soil macroporosity and microporosity based on sand content and bulk density. Rev. Bras. Ciencias do Solo 35, 447–459.

Sus, O., Poyatos, R., Barba, J., Carvalhais, N., Llorens, P., Williams, M., Vilalta, J.M., 2014. Time variable hydraulic parameters improve the performance of a mechanistic stand transpiration model. A case study of Mediterranean Scots pine sap flow data assimilation. Agric. For. Meteorol. 198-199, 168–180. doi:10.1016/j.agrformet.2014.08.009

Tague, C.L., McDowell, N.G., Allen, C.D., 2013. An integrated model of environmental effects on growth, carbohydrate balance, and mortality of Pinus ponderosa forests in the southern Rocky Mountains. PLoS One 8. doi:10.1371/journal.pone.0080286

Tesfa, T.K., Tarboton, D.G., Chandler, D.G., McNamara, J.P., 2009. Modeling soil depth from topographic and land cover attributes. Water Resour. Res. 45, W10438. doi:10.1029/2008WR007474

Vayreda, J., Martinez-Vilalta, J., Gracia, M., Retana, J., 2012. Recent climate changes interact with stand structure and management to determine changes in tree carbon stocks in Spanish forests. Glob. Chang. Biol. 18, 1028–1041. doi:10.1111/j.1365-2486.2011.02606.x

Vicente-Serrano, S.M., Beguería, S., López-Moreno, J.I., 2010. A multiscalar drought index sensitive to global warming: the Standardized Precipitation Evapotranspiration Index. J. Clim. 23, 1696–1718. doi:10.1175/2009JCLI2909.1

Vilà-Cabrera, A., Martínez-Vilalta, J., Vayreda, J., Retana, J., 2011. Structural and climatic determinants of demographic rates of Scots pine forests across the Iberian Peninsula. Ecol. Appl. 21, 1162–1172.

Villaescusa, R., Díaz, R., 1998. Segundo inventario forestal nacional (1986–1996). Ministerio de Medio Ambiente, ICONA, Madrid.

Villanueva, J.A., 2004. Tercer inventario forestal nacional (1997–2007). Ministerio de Medio Ambiente y Medio Rural, ICONA, Madrid.

Weissteiner, C.J., Boschetti, M., Böttcher, K., Carrara, P., Bordogna, G., Brivio, P.A., 2011. Spatial explicit assessment of rural land abandonment in the Mediterranean area. Glob. Planet. Change 79, 20–36. doi:10.1016/j.gloplacha.2011.07.009

Weltzin, J.F., Loik, M.E., Schwinning, S., Williams, D.G., Fay, P.A., Haddad, B.M., Harte, J., Huxman, T.E., Knapp, A.K., Lin, G., Pockman, W.T., Shaw, M.R., Small, E.E., Smith, M.D., Smith, S.D., Tissue, D.T., Zak, J.C., 2003. Assessing the response of terrestrial ecosystems to potential changes in precipitation. Bioscience 53, 941–952. doi:10.1641/0006-3568(2003)053[0941:ATROTE]2.0.CO;2

Zavala, M.A., Bravo de la Parra, R., 2005. A mechanistic model of tree competition and facilitation for Mediterranean forests: Scaling from leaf physiology to stand dynamics. Ecol. Modell. 188, 76–92. doi:10.1016/j.ecolmodel.2005.05.006

Zheng, D., Hunt Jr, E.R., Running, S.W., 1996. Comparison of available soil water capacity estimated from topography and soil series information. Landsc. Ecol. 11, 3–14.

Supplementary material

Additional Supporting Information may be found in the online version of this article:

Appendix S1 Detailed description of the water balance model.

Appendix S2 Model sensitivity analyses.

Appendix S3 Details of the calibration of species-specific parameters.

Appendix S4 Supplementary figures.

As a service to our authors and readers, this journal provides supporting information supplied by the authors. Such materials are peer-reviewed and may be reorganized for online delivery, but are not copy-edited or typeset. Technical support issues arising from supporting information (other than missing files) should be addressed to the authors.

Fig.1

Click here to download high resolution image

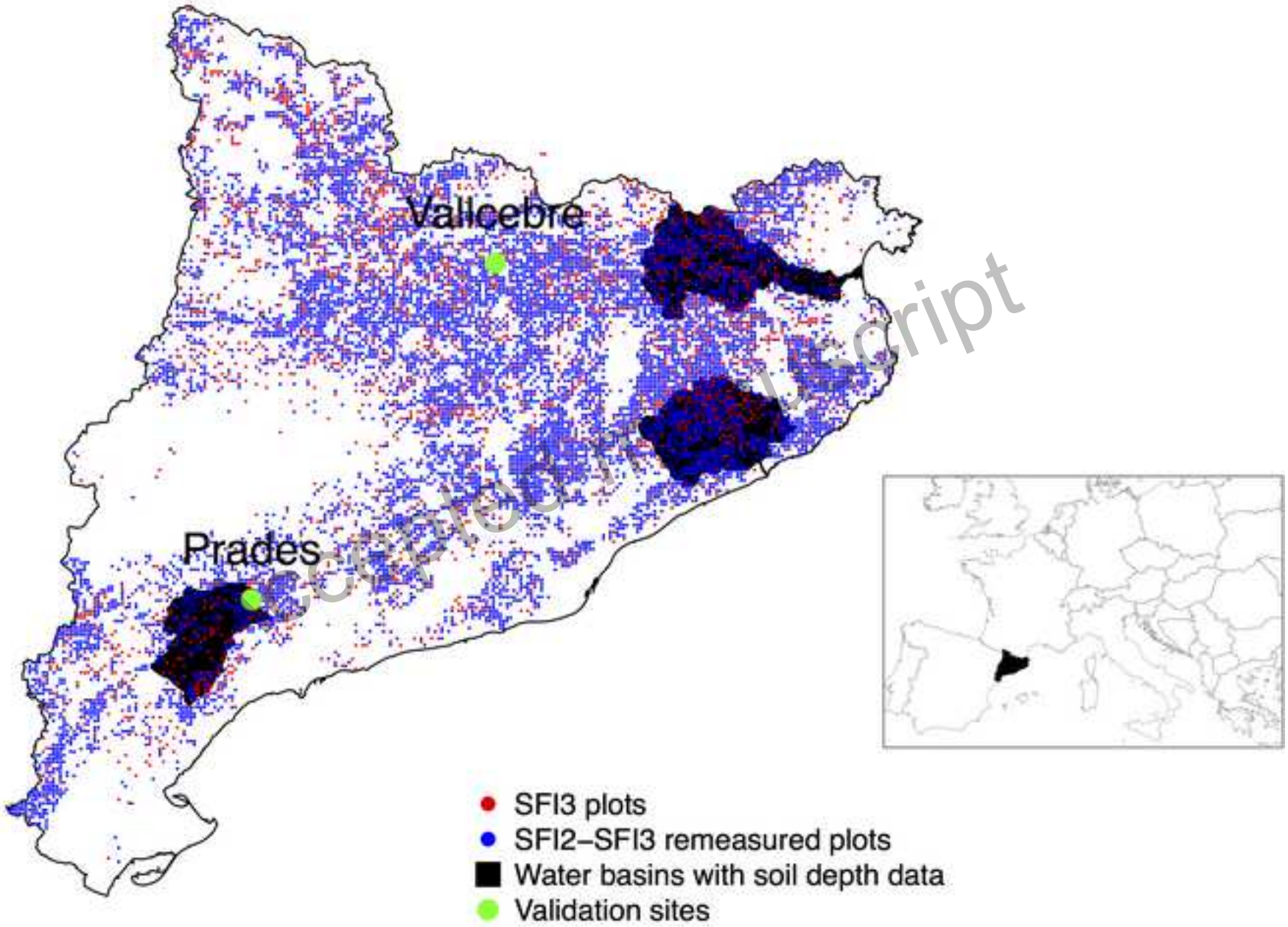

Fig.2a

Click here to download high resolution image

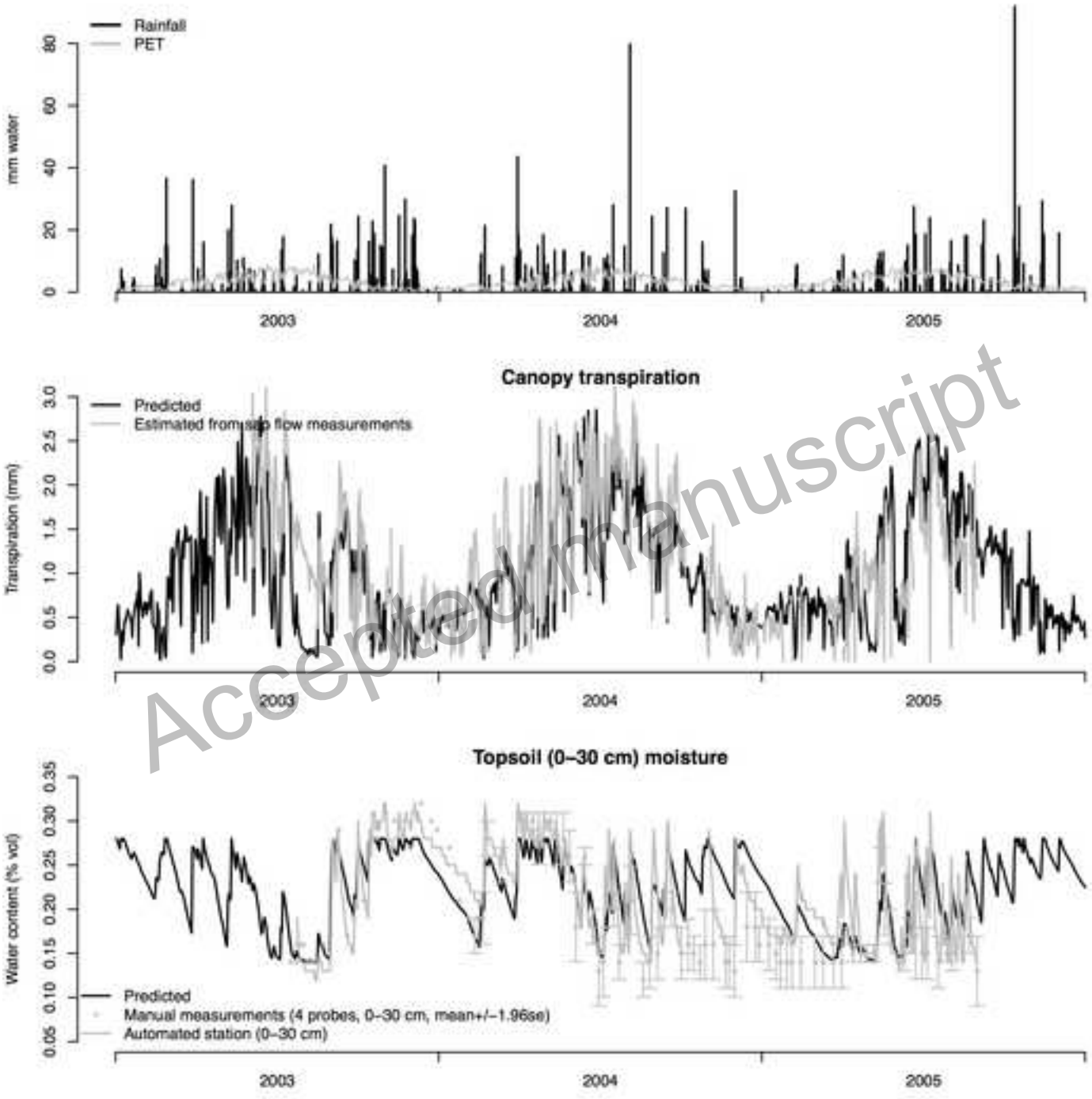

Fig.2b

Click here to download high resolution image

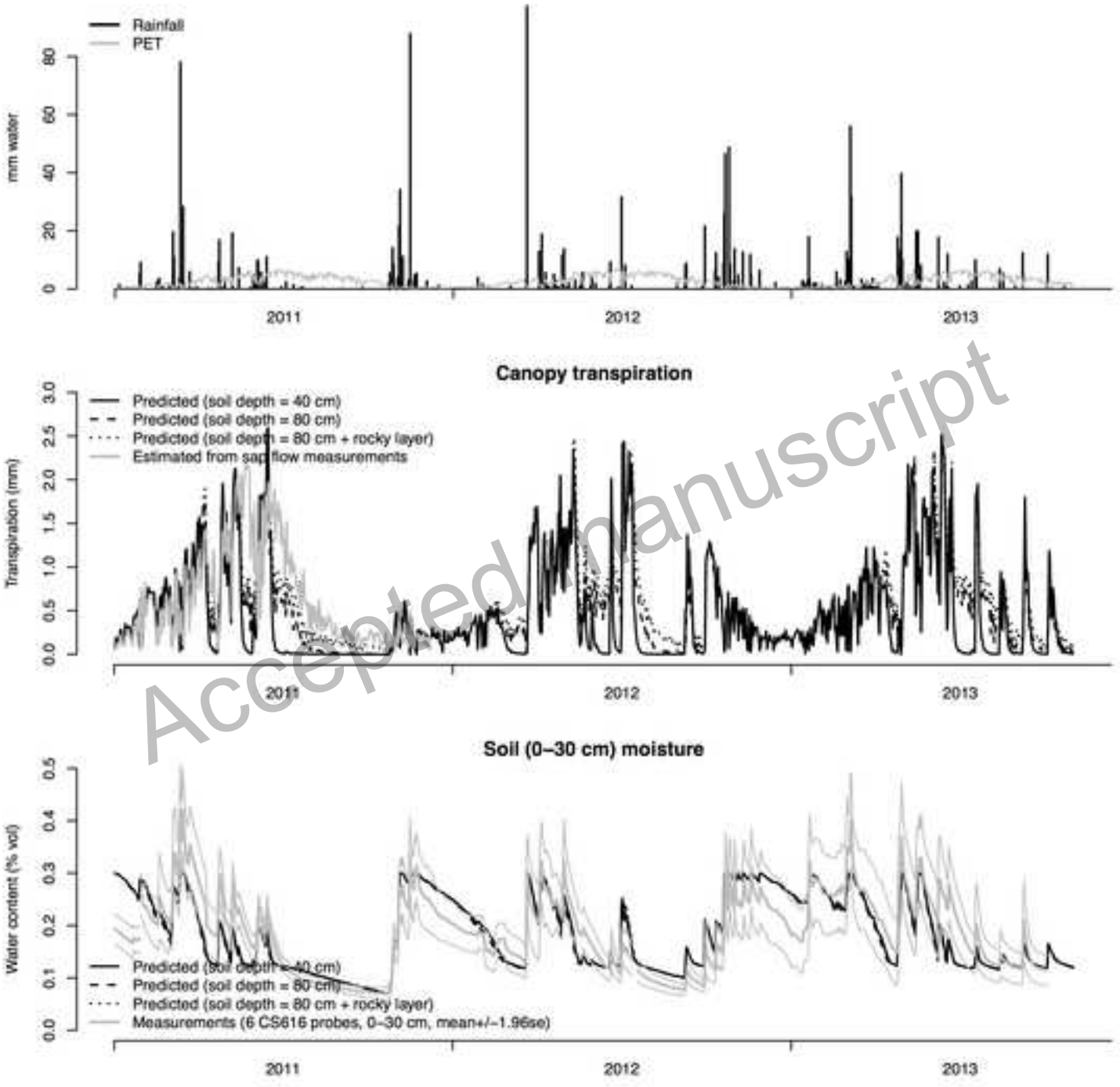

Fig. 3a
Click here to download high resolution image

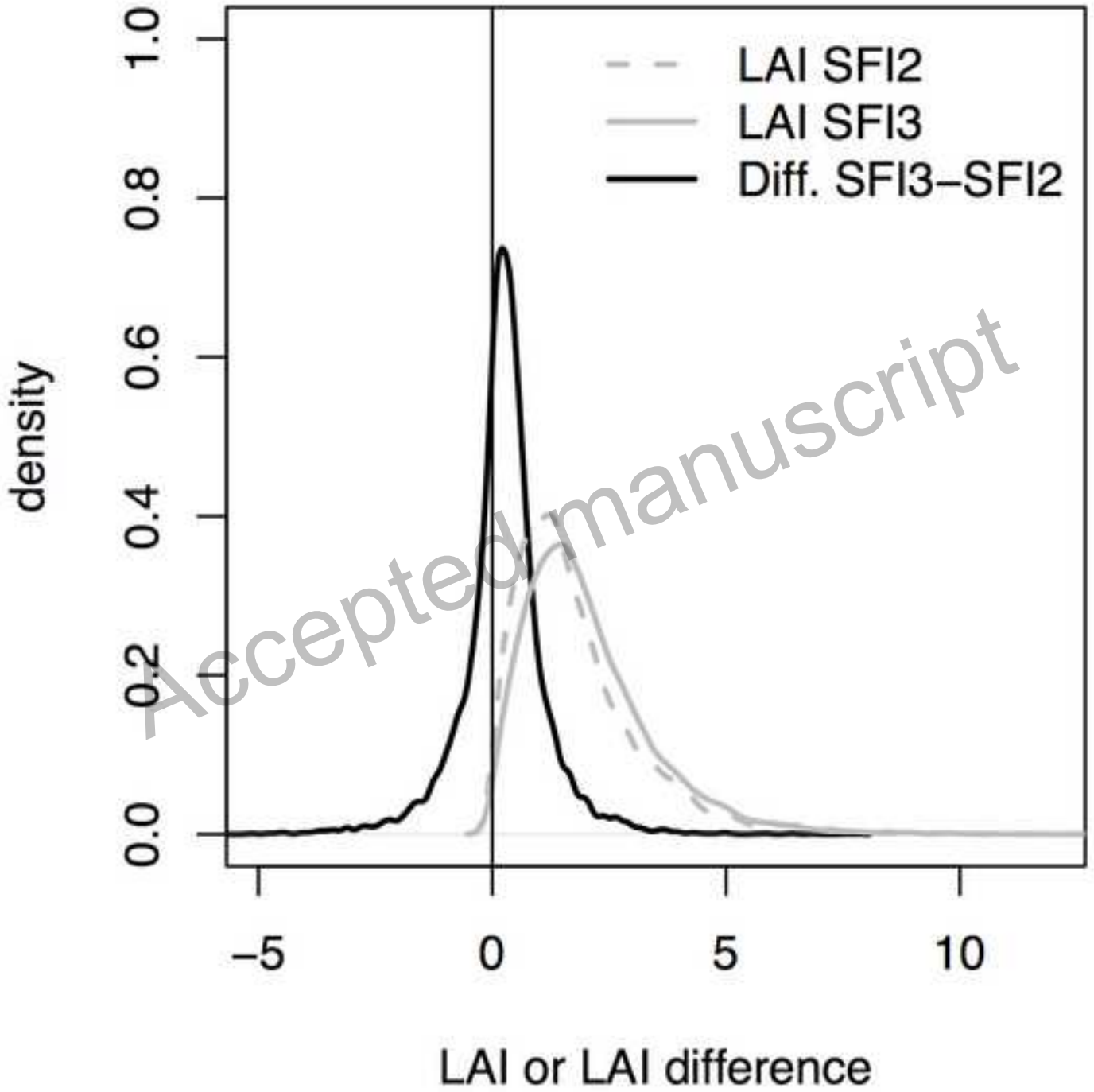

Fig. 3b

Click here to download high resolution image

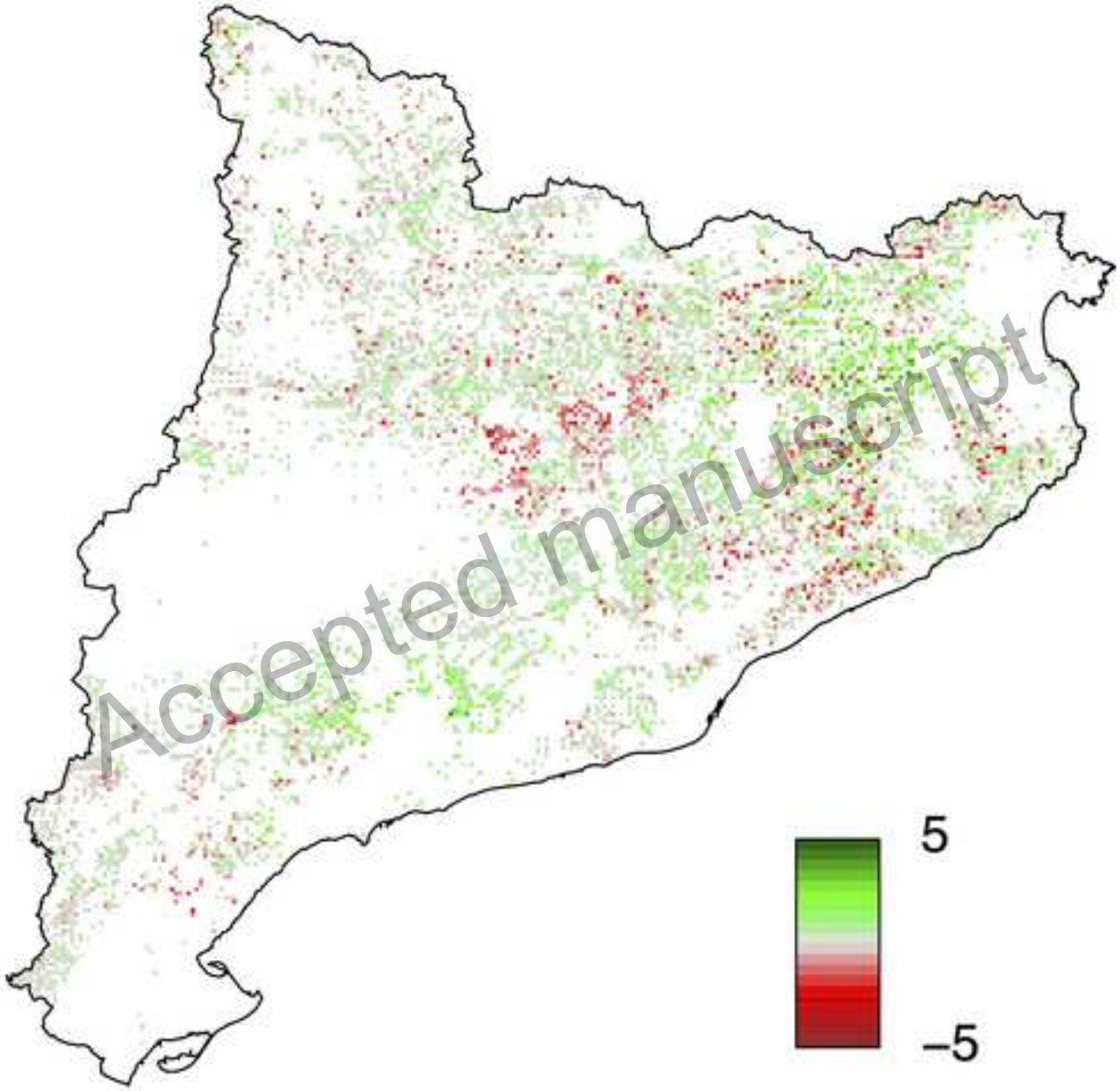

Fig. 4

Click here to download high resolution image

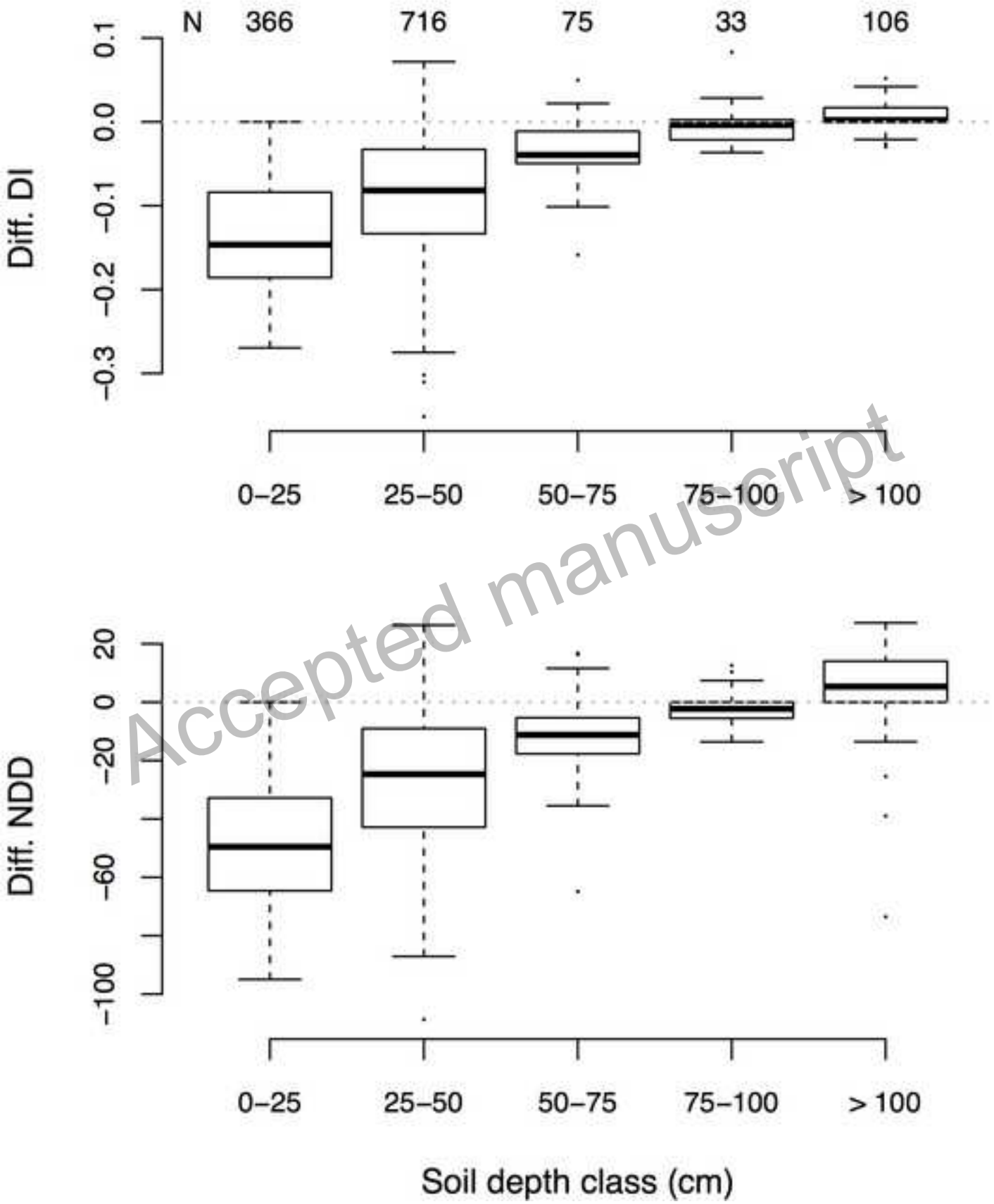

Fig. 5

Click here to download high resolution image

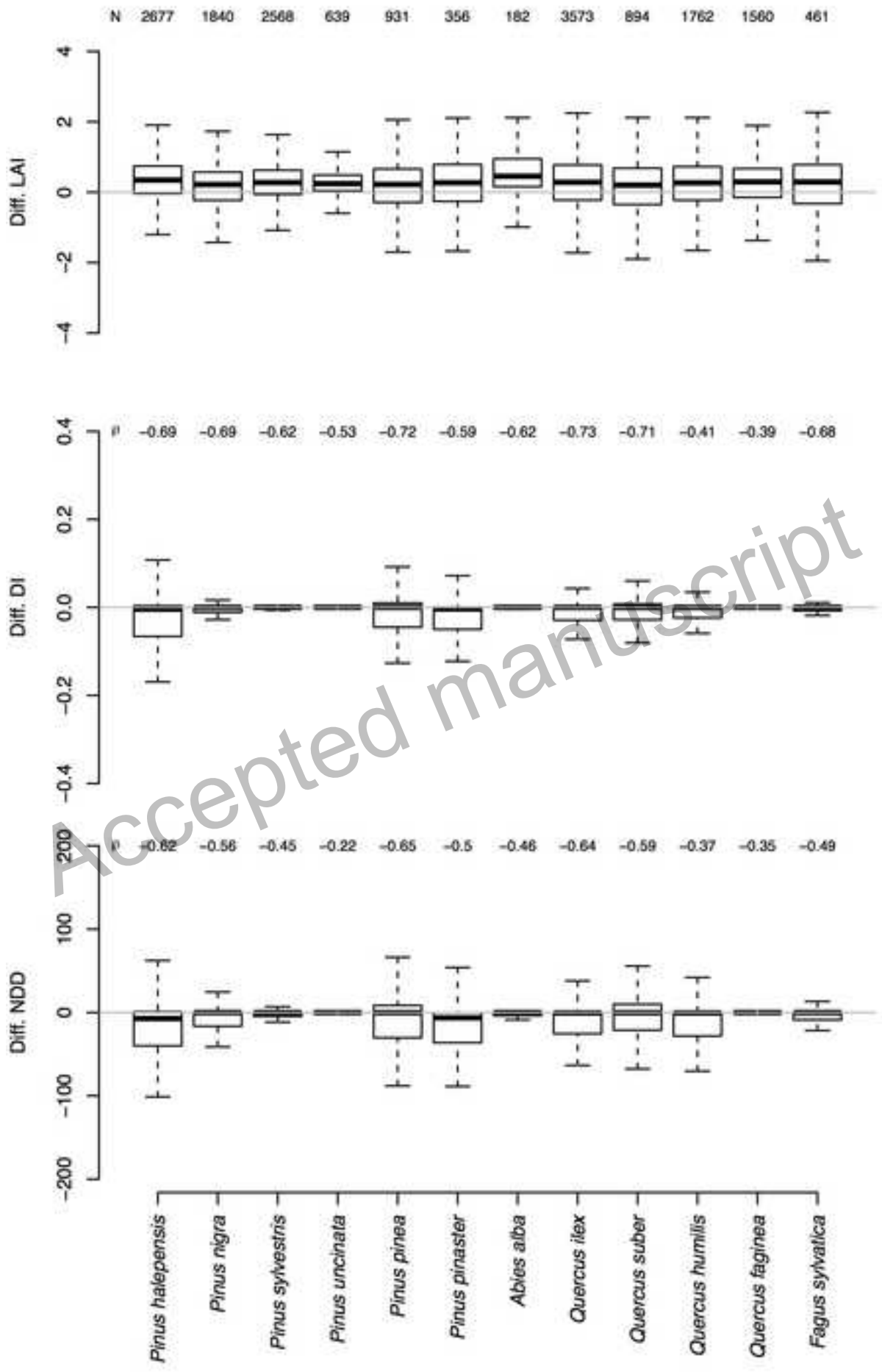

Fig. 6a

Click here to download high resolution image

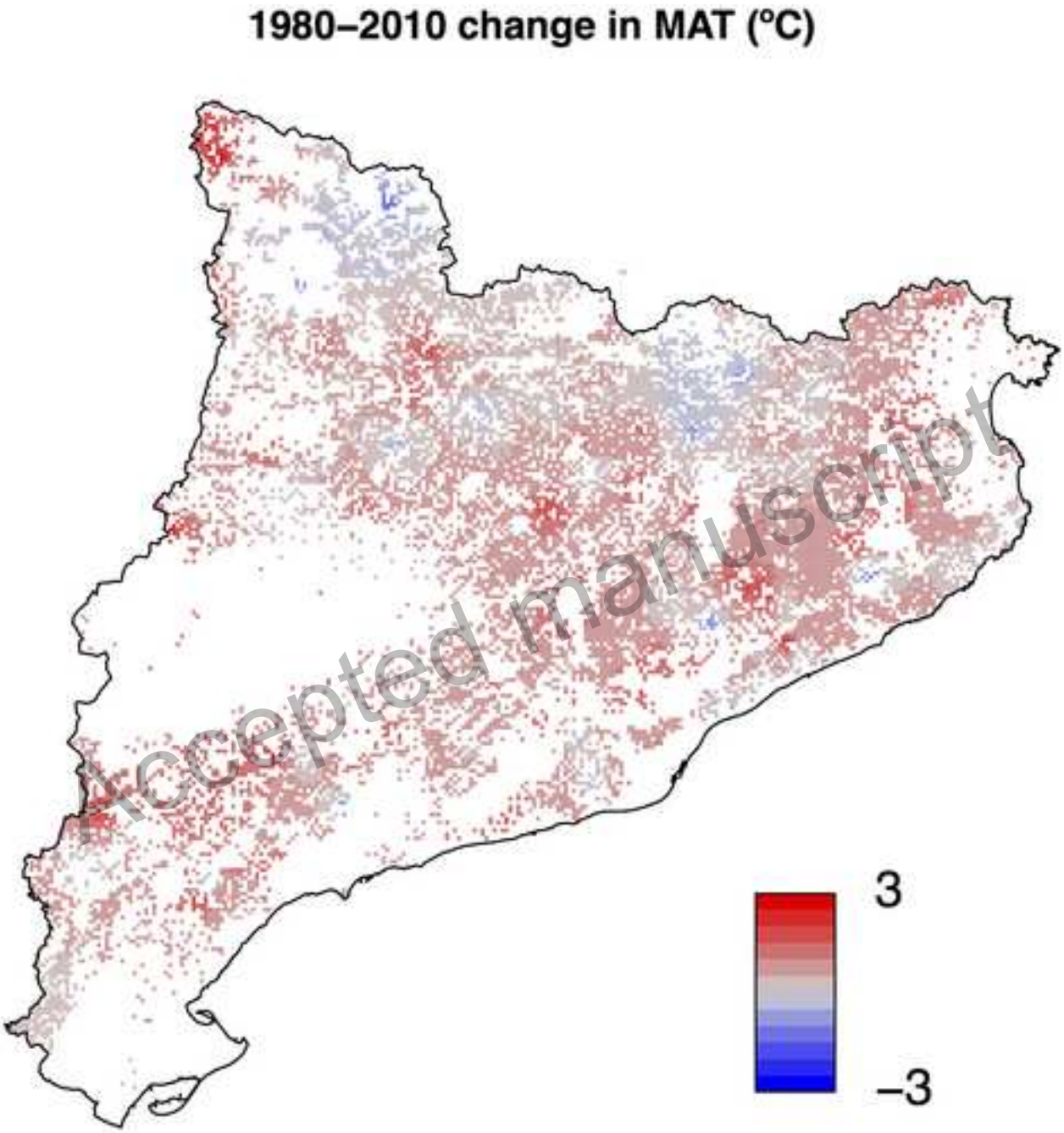

Fig. 6b

Click here to download high resolution image

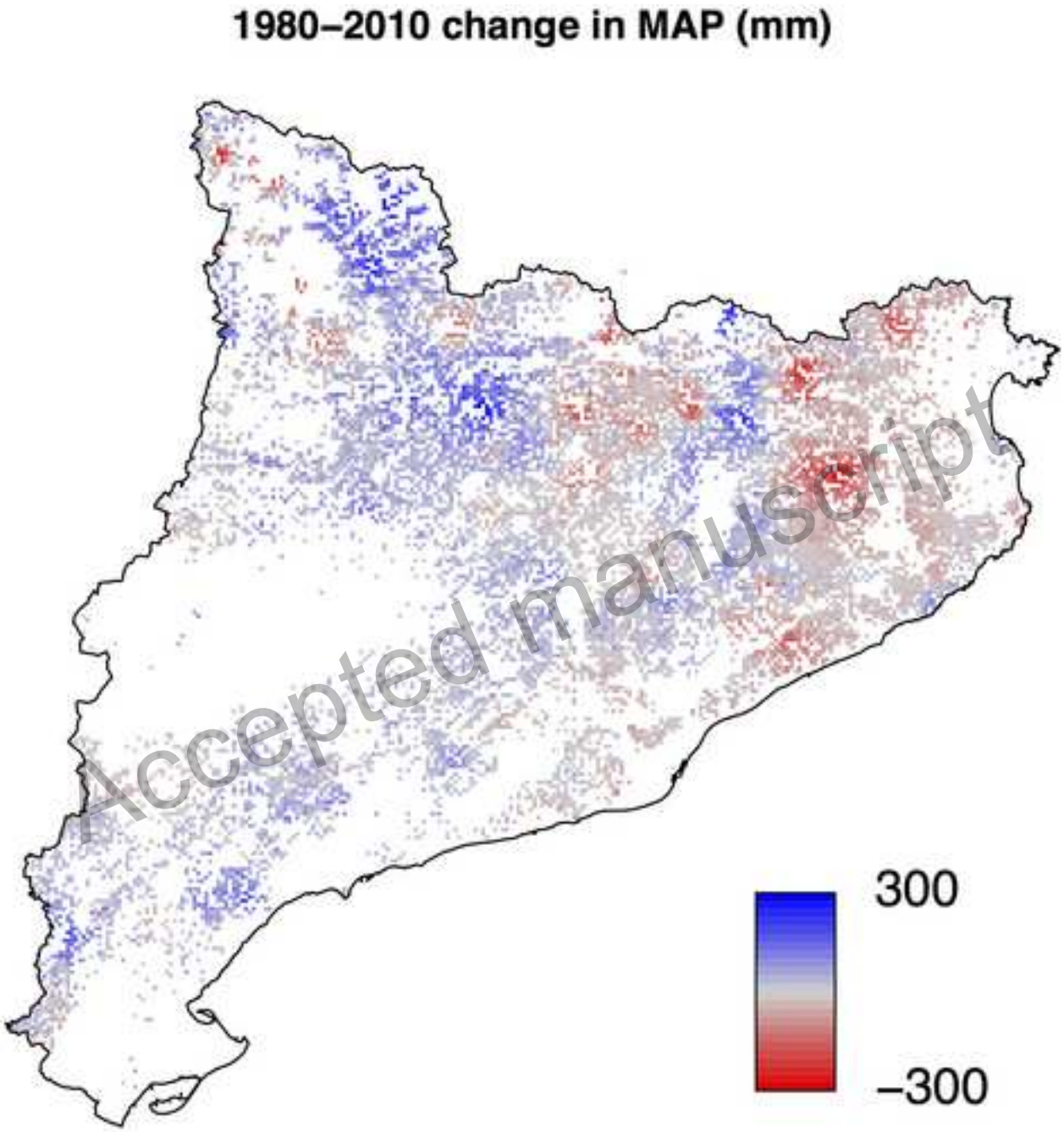

Fig. 6c
Click here to download high resolution image

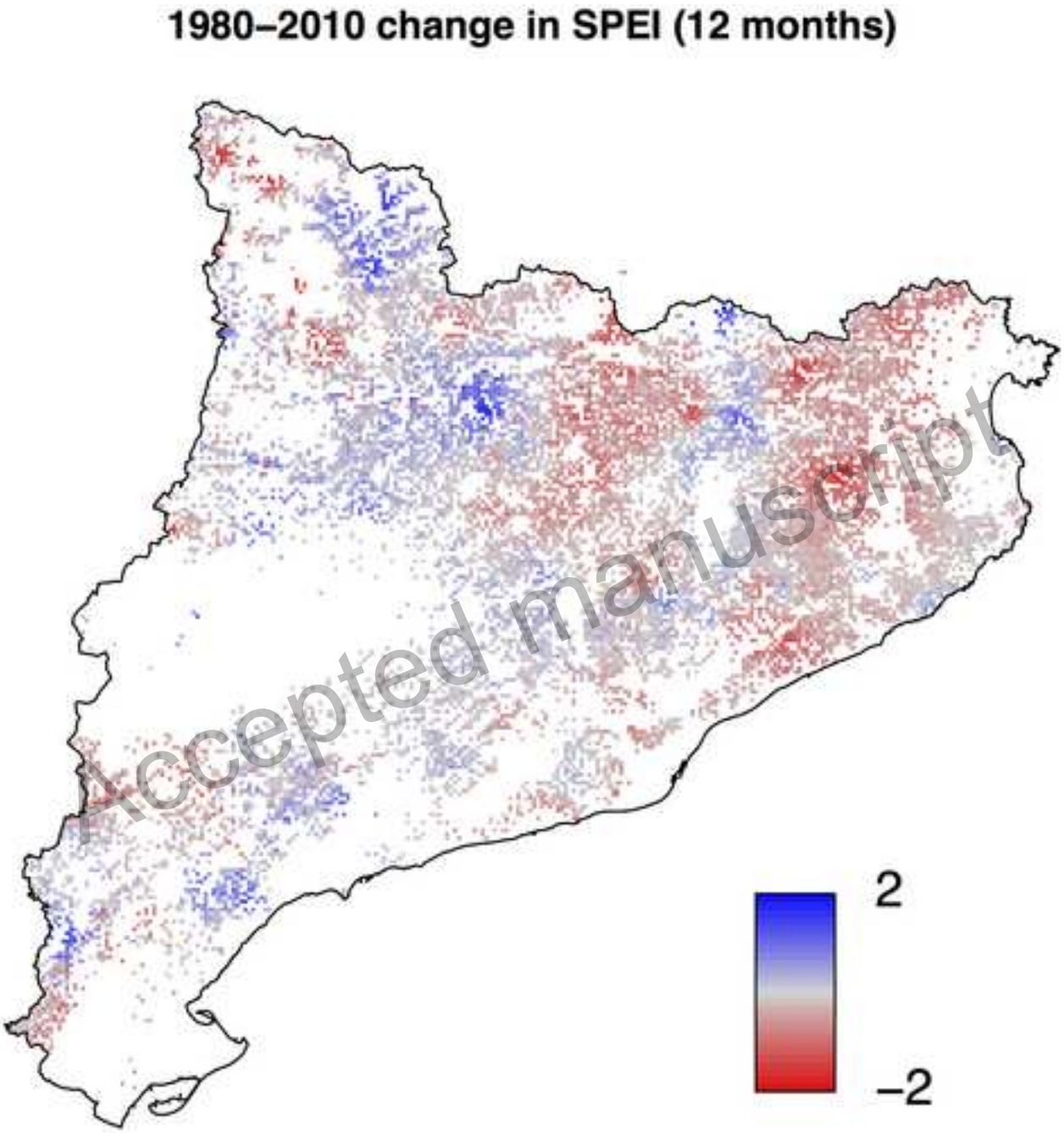

Fig. 7

Click here to download high resolution image

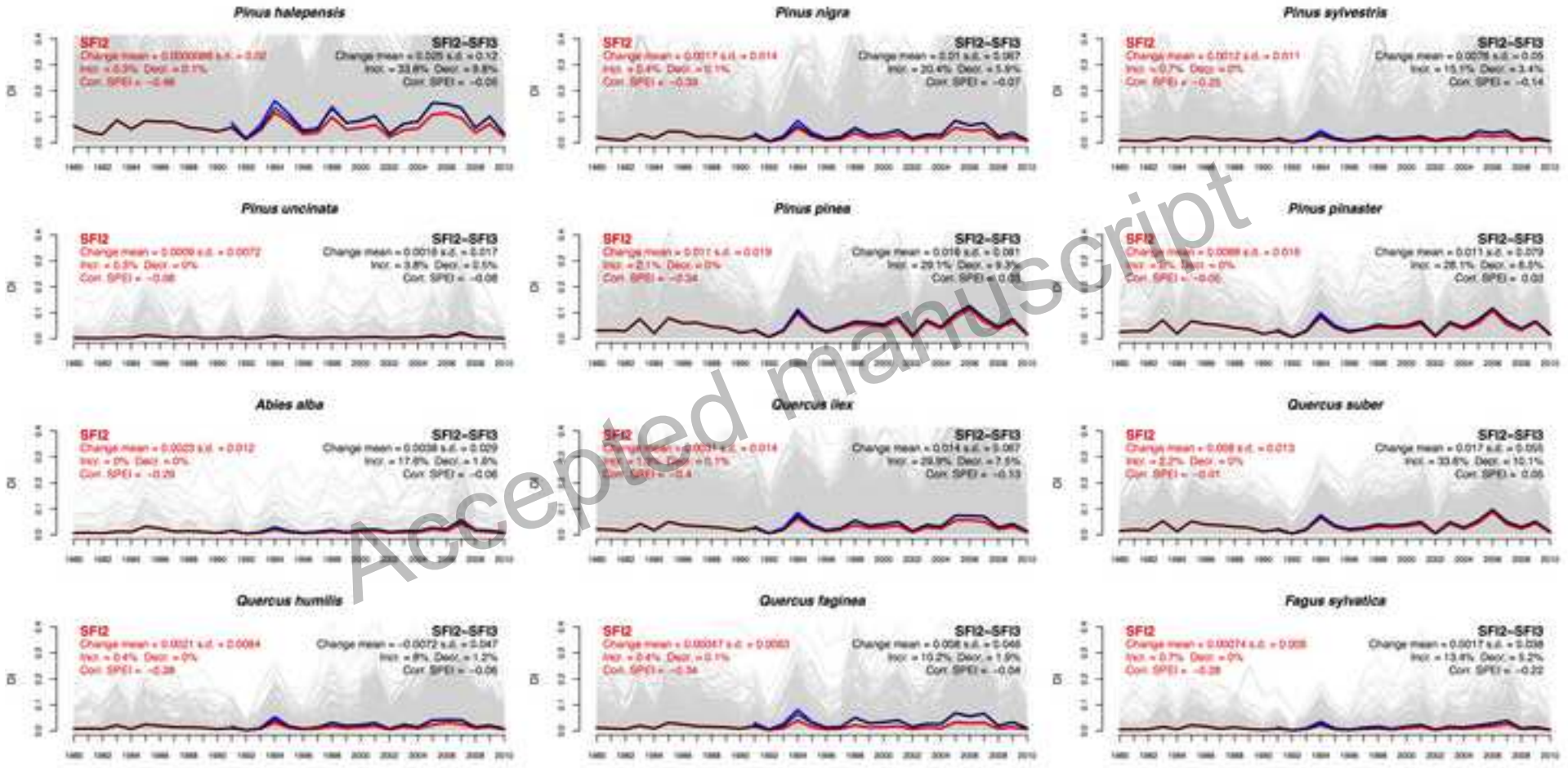

Fig. 8

Click here to download high resolution image

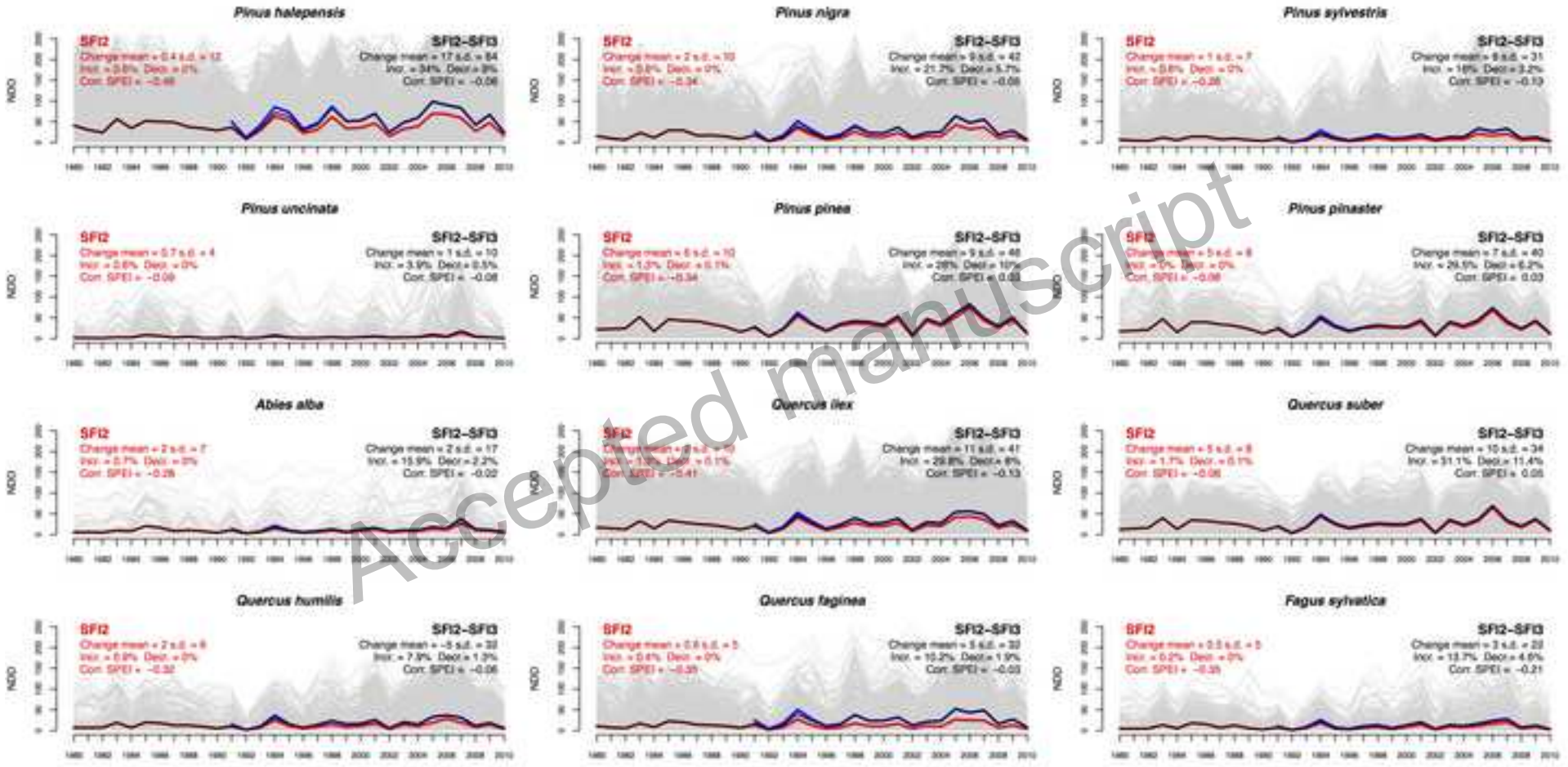

Supplementary Material S1

Click here to download Supplementary Interactive Plot Data (CSV): Appendix_S1_ModelDetails_Revised.docx

Supplementary Material S2

Click here to download Supplementary Interactive Plot Data (CSV): Appendix_S2_Sensitivity analyses_Revised.docx

Supplementary Material S3

Click here to download Supplementary Interactive Plot Data (CSV): Appendix_S3_Calibration_Revised.docx

Supplementary Material S4

Click here to download Supplementary Interactive Plot Data (CSV): Appendix_S4_SupplementaryFigures_Revised.docx